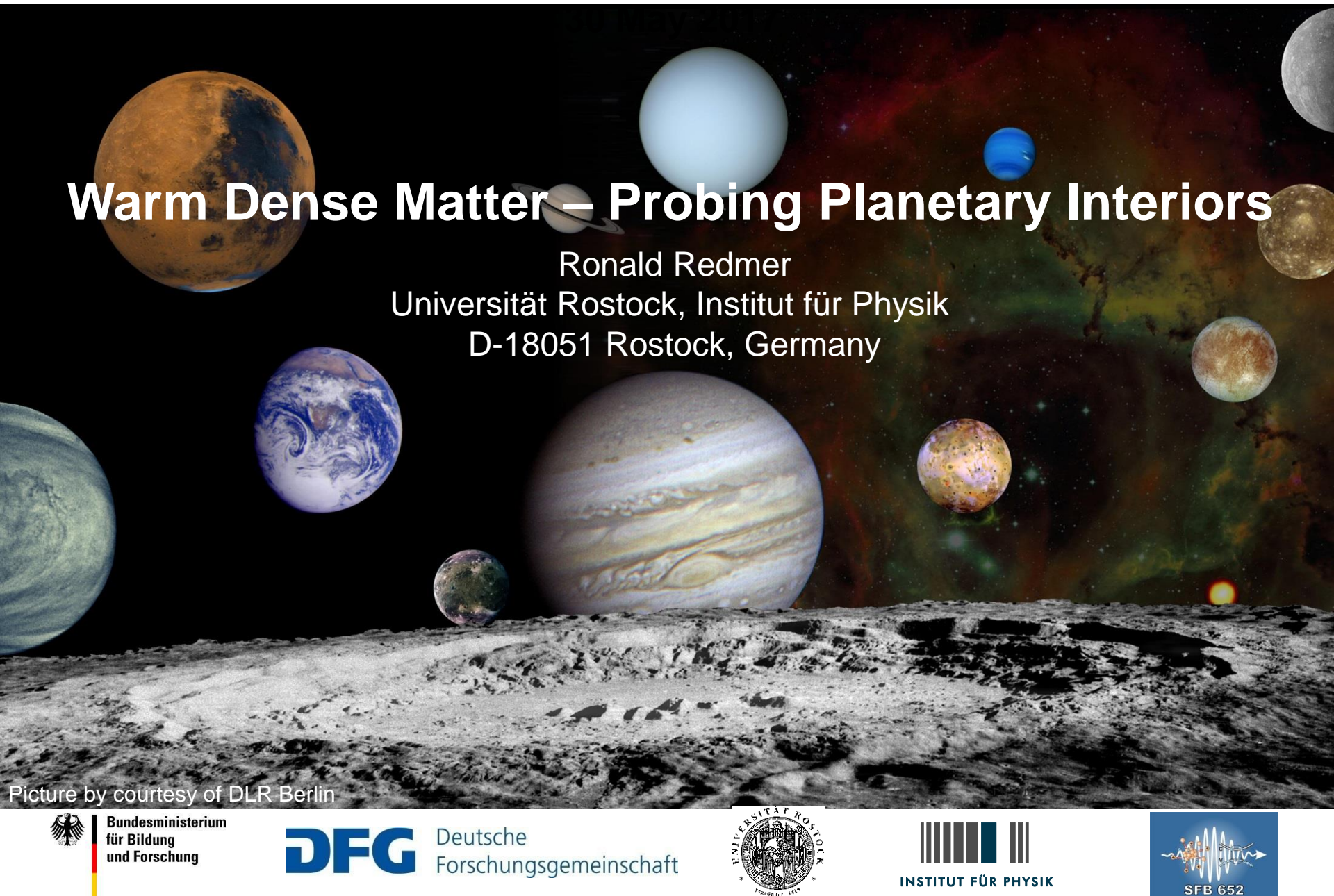


Warm Dense Matter – Probing Planetary Interiors

Ronald Redmer

Universität Rostock, Institut für Physik
D-18051 Rostock, Germany



Picture by courtesy of DLR Berlin



Bundesministerium
für Bildung
und Forschung



Deutsche
Forschungsgemeinschaft



Acknowledgements



SFB 652
BMBF FSP 301
BMBF FSP 302
DFG SPP 1385
DFG SPP 1488
FOR 2440
HLRN



Andreas Becker
Mandy Bethkenhagen
Richard Bredow
Daniel Cebulla
Martin French
Clemens Kellermann
Nadine Nettelmann
Kai-Uwe Plagemann
Martin Preising
Ludwig Scheibe
Manuel Schöttler
Philipp Sperling
Bastian Witte
Thomas Bornath
Wolf Kraeft



Contents

1. Introduction: Warm Dense Matter

Exoplanets

Planetary Interiors

High-Pressure Experiments

2. DFT-MD Simulations

3. Results

H-He: Jupiter (Saturn)

C-N-O-H: Uranus and Neptune

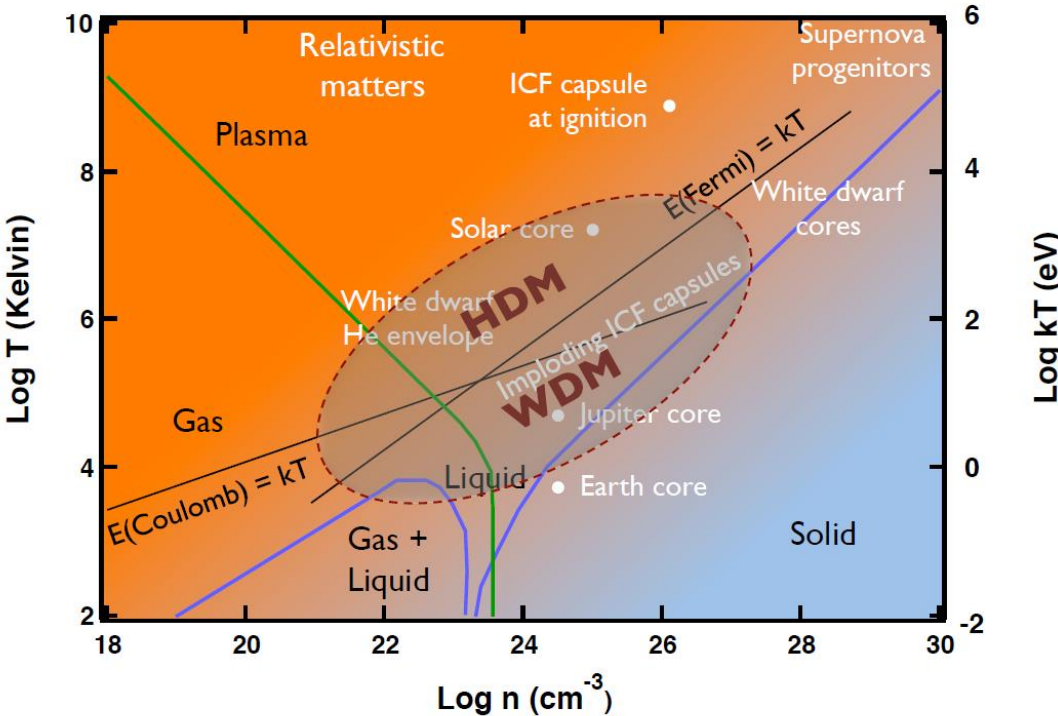
MgO-FeO-SiO₂: Rocky Planets

4. Outlook

Warm Dense Matter (WDM)

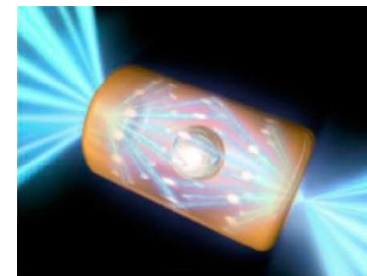
See: Basic Research Needs for High Energy Density Laboratory Physics (DOE Office of Science and NNSA, 2010)

High Energy Density Universe



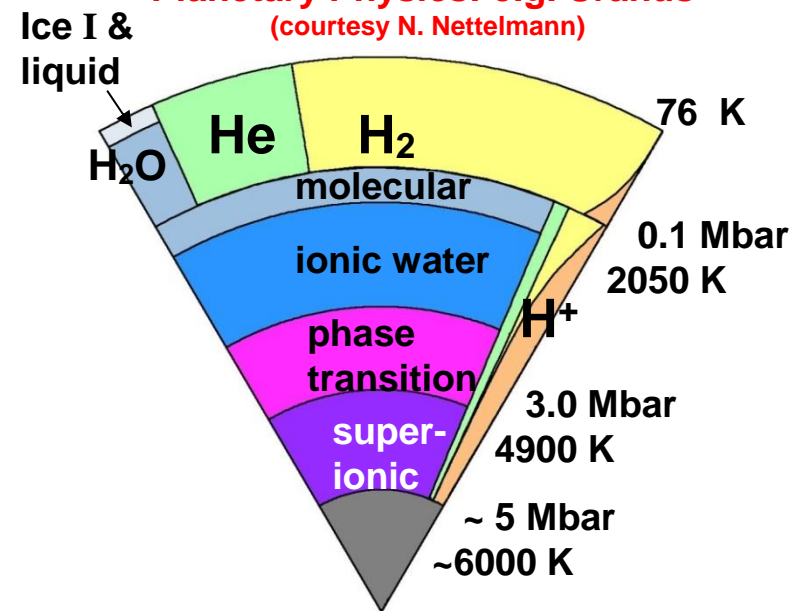
DENSITY ~ solid density (0.1 – 10)
 TEMPERATURE ~ few eV
 PRESSURES ~ Mbar-Gbar

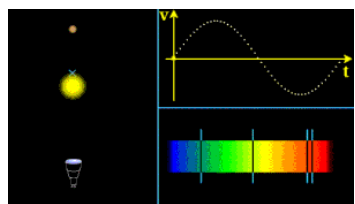
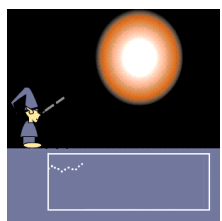
Inertial Confinement Fusion
 (courtesy NIF)



$T > 10^8 \text{ K}$
 $P > 100 \text{ Gbar}$

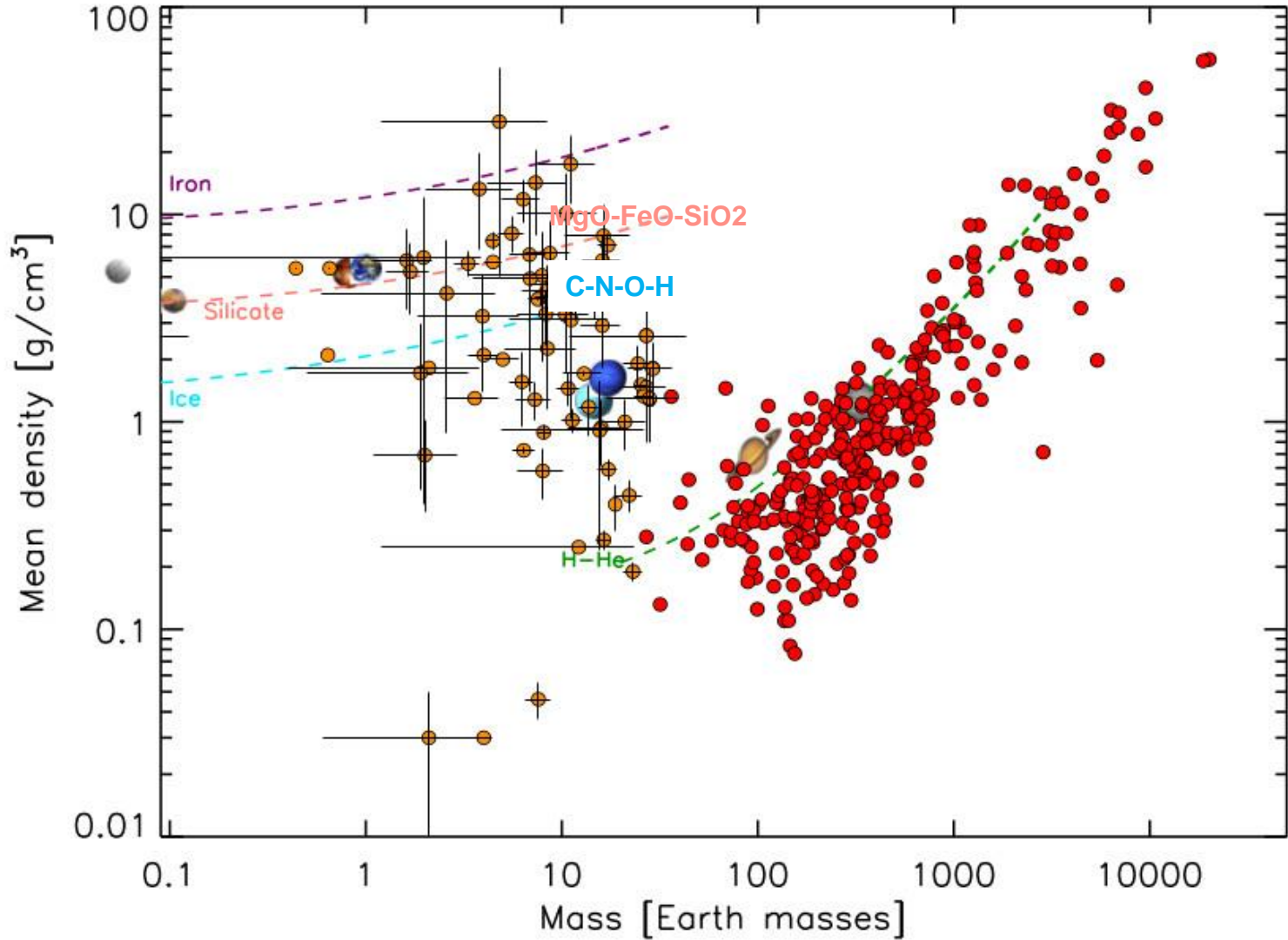
Planetary Physics: e.g. Uranus
 (courtesy N. Nettelmann)





Mean Density vs. Mass

H. Rauer et al., Exp. Astron. **38**, 249 (2014)



Kepler-22 System

G5 star, 600 Ly away

Solar System

Habitable Zone

$R \sim 2.4 R_E$
 $T \sim 290$ d



Kepler-22b



Mercury



Venus



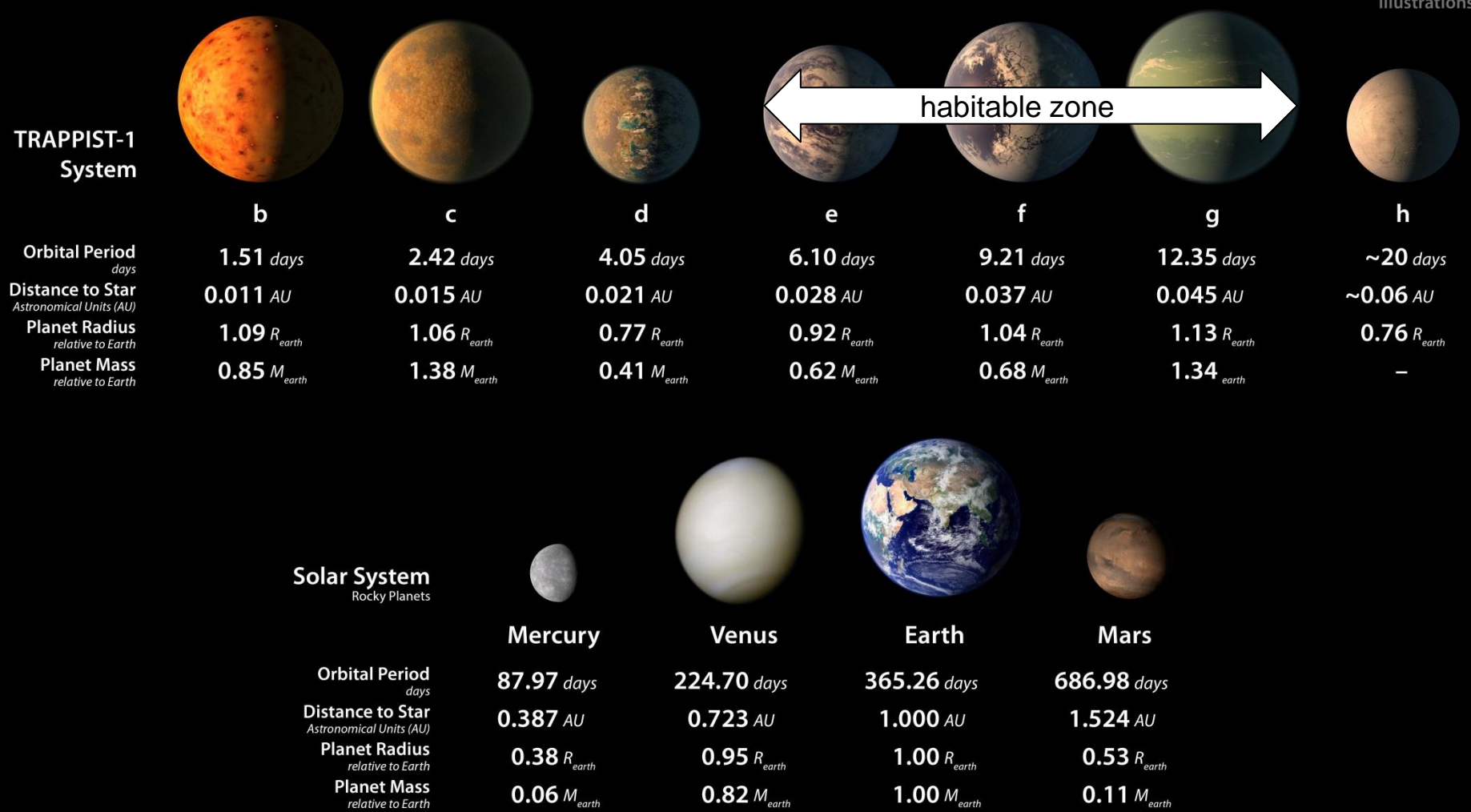
Earth



Mars

Planets and orbits to scale

M8 star: 40 Ly away, $0.082 M_{\text{Sun}}$



Transiting Planets and Planetesimals Small Telescope (TRAPPIST),
La Silla Observatory, Chile: M. Gillon et al., Nature **542**, 456 (2017)

Basic Equations for Planetary Modeling

mass conservation:

$$dm = 4\pi r^2 \rho(r) dr$$

hydrostatic equation of motion:

$$\frac{1}{\rho} \frac{dP}{dr} = \frac{dU}{dr}, \quad U = V + Q$$

gravitational potential:

$$V(\vec{r}) = -G \int_{V_0} d^3 r' \frac{\rho(r')}{|\vec{r} - \vec{r}'|}$$

expansion into Legendre polynomials:

$$V(r, \theta) = -\frac{GM}{r(\theta)} \left(1 - \sum_{i=1}^{\infty} \left(\frac{R_{eq}}{r(\theta)} \right)^{2i} J_{2i} P_{2i}(\cos \theta) \right)$$

gravitational moments:

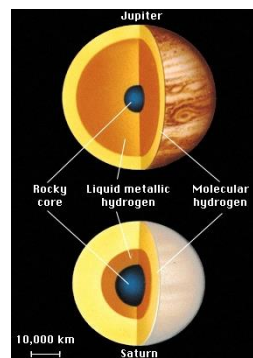
$$J_{2i} = -\frac{1}{MR_{eq}^{2i}} \int d^3 r' \rho(r'(\theta')) r'^{2i} P_{2i}(\cos \theta')$$

Calculations via theory of figures (Zharkov & Trubitsyn)
with boundary conditions $M_p(R_p)$, Y_1 , \bar{Y} , P and T at 1 bar.

**Mass distribution along (piecewise) isentropes/isotherms
according to EOS data for WDM – most important input!**

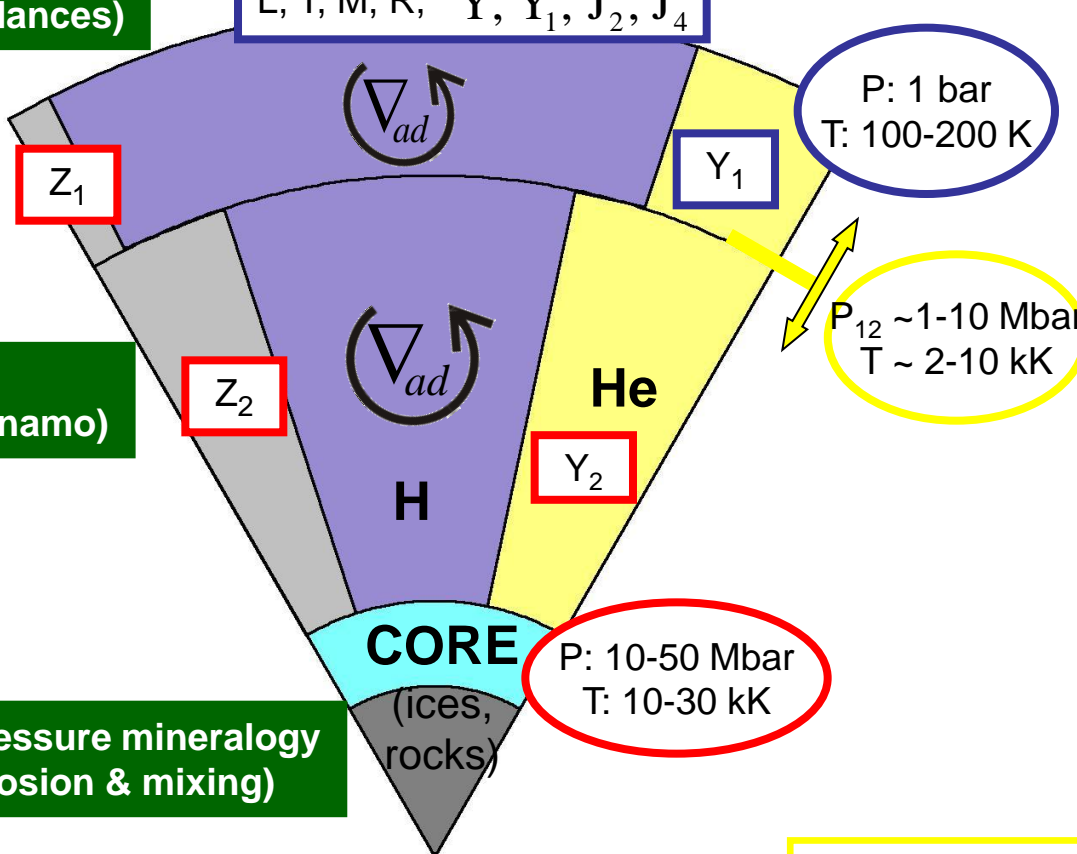
Interior of Gas Giants: H-He

Three-layer model, input and constraints



Atmosphere models
(luminosity, abundances)

$L, T, M, R, \bar{Y}, Y_1, J_2, J_4$



Magnetic field generation (dynamo)

High-pressure mineralogy
(core erosion & mixing)

Physical origin and location of the layer boundary:
→ MIT (PPT)
→ H-He demixing

- constraints
- results from modeling
- free parameter

Matter under extreme conditions (WDM):

- High-pressure H-He phase diagram
- EOS of complex mixtures
- Electrical & thermal conductivity
- Diffusion & viscosity

Interior of Jupiter: Juno Mission

High-precision measurement of gravitational moments J_{2i}



See e.g.

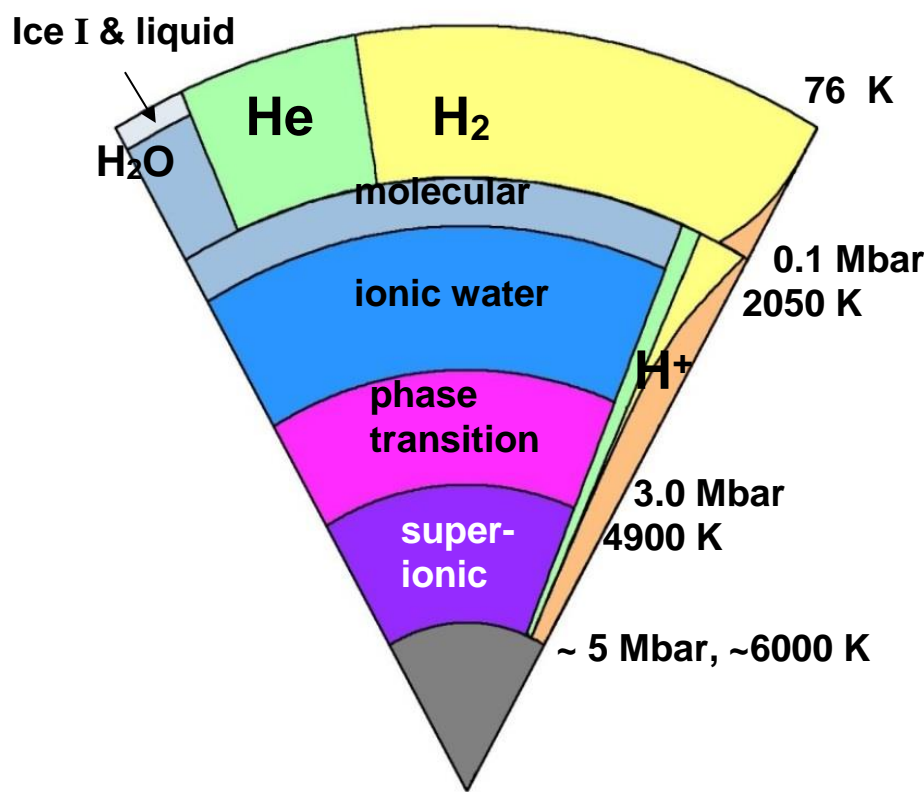
W.B. Hubbard and B. Militzer, ApJ **820**, 80 (2016)

S. Wahl et al., J. Geophys. Res. **44**, 4649 (2017)

N. Nettelmann, A&A **606**, A139 (2017)

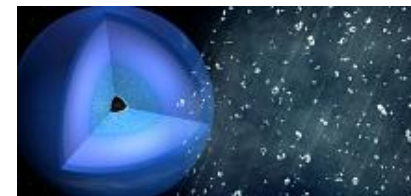
Interior of Ice Giants: C-N-O-H Mixture

Multi-layer models



U & N
Neptune-like exos
mini-Neptunes

Physical origin and location of layer boundaries:
→ ice phase diagram
→ superionic phase?
→ carbon rain?
→ solubility of rock material?
→ inhomogeneous zone from formation:
thermal boundary layer?



D. Kraus et al.,
Nat. Astron.
1, 606 (2017)

Interior structure models of this type are not uniquely defined.
Accurate EOS data for warm dense C-N-O-H-He mixtures are
needed and information on the high-P phase diagram.

See e.g. Hubbard et al. (1980, 89, 95), Helled et al. (2009, 10, 11), Nettelmann et al. (2013)

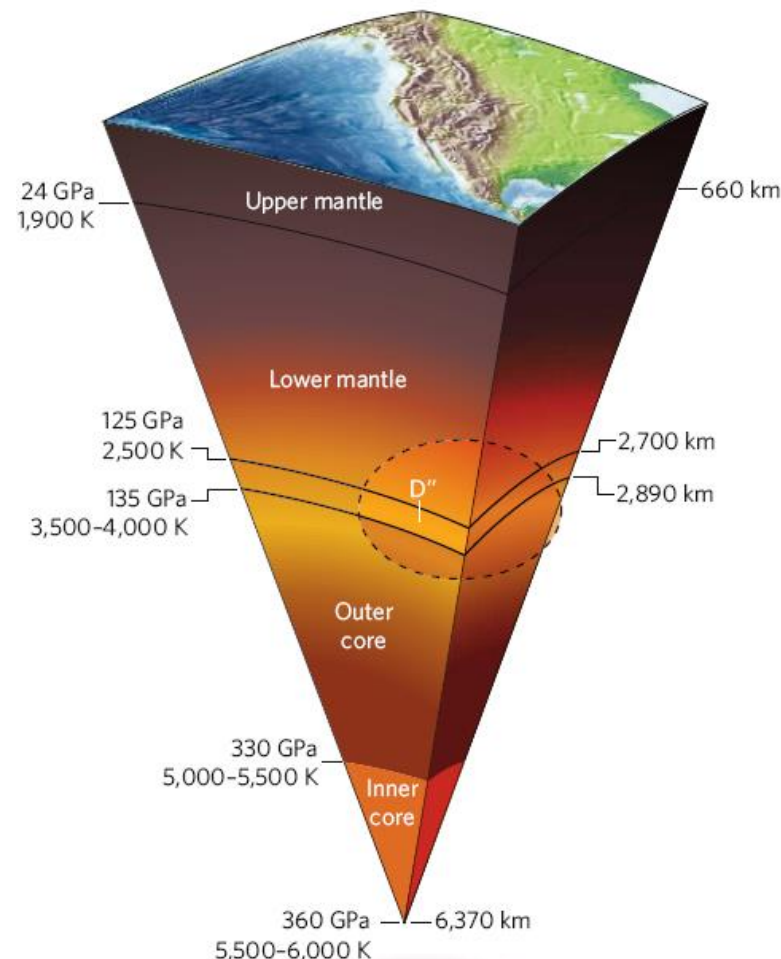
From Earth to Super-Earths – Mineralogy at the Extreme

Upper mantle: olivine $(\text{Mg}, \text{Mn}, \text{Fe})_2[\text{SiO}_4]$

Lower mantle: perovskite MgSiO_3 , PPv

Core: $(\text{Fe}, \text{Ni})[\text{Si}, \text{O}, \text{S}, \text{C} \dots]$ – melting line, dynamo

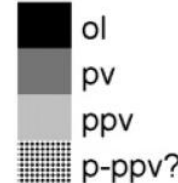
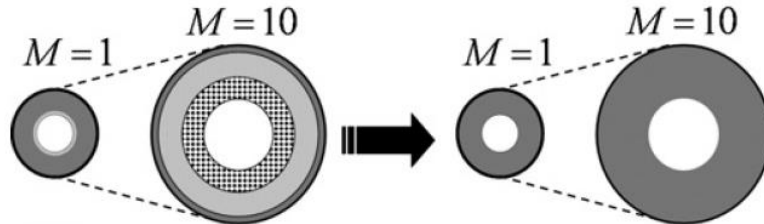
Super Earths $1-10 M_E$
Kepler, CoRoT, PLATO 2.0
Completely different?



V. Stamenkovic et al., Icarus 216, 572 (2011)

Expected structure

Simplified Model



$M [M_{\text{Earth}}]$	1	5	10
$P^{cmb} [\text{GPa}]$	135	570	1100

High-P crystal structures?
High-P EOS data and phase diagram?
Slope of melting line?
Electrical and thermal conductivity?
Viscosity?

Diamond Anvil Cells (DACs)

Conventional DAC technique is limited to static pressures of few Mbar and low T using resistive or pulsed laser heating.

Dynamic dDAC (for molecular solids) > 2 Mbar

Evans et al. 2007

Double-stage dsDAC – potential to reach 10 Mbar

Dubrovinsky et al. 2012: Re >6 Mbar

Dubrovinsky et al. 2015: Os ~8 Mbar

X-ray diagnostics at 3rd generation synchrotrons:

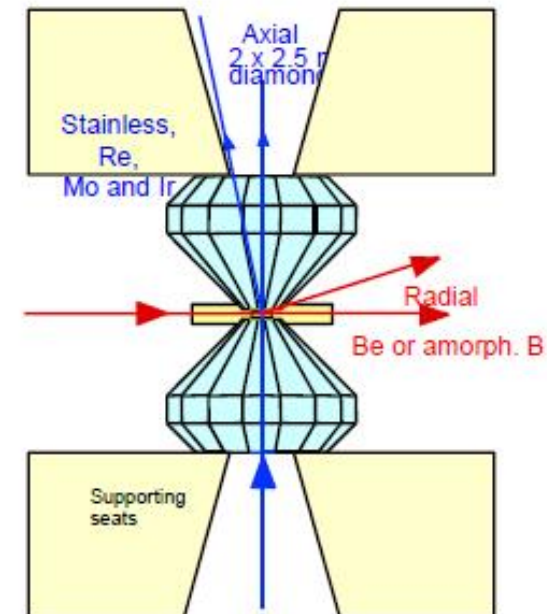
- ESRF, ECB@PETRA III, APS, Diamond ...
- Structure, phase transitions, EOS, reflectivity ...

Laser-driven shocks: NIF, Omega, Nike ... Orion, Vulcan, LMJ, LULI, PeTAL, Phelix ...

Combination of pre-compressed samples (DACs) and shock waves (lasers)

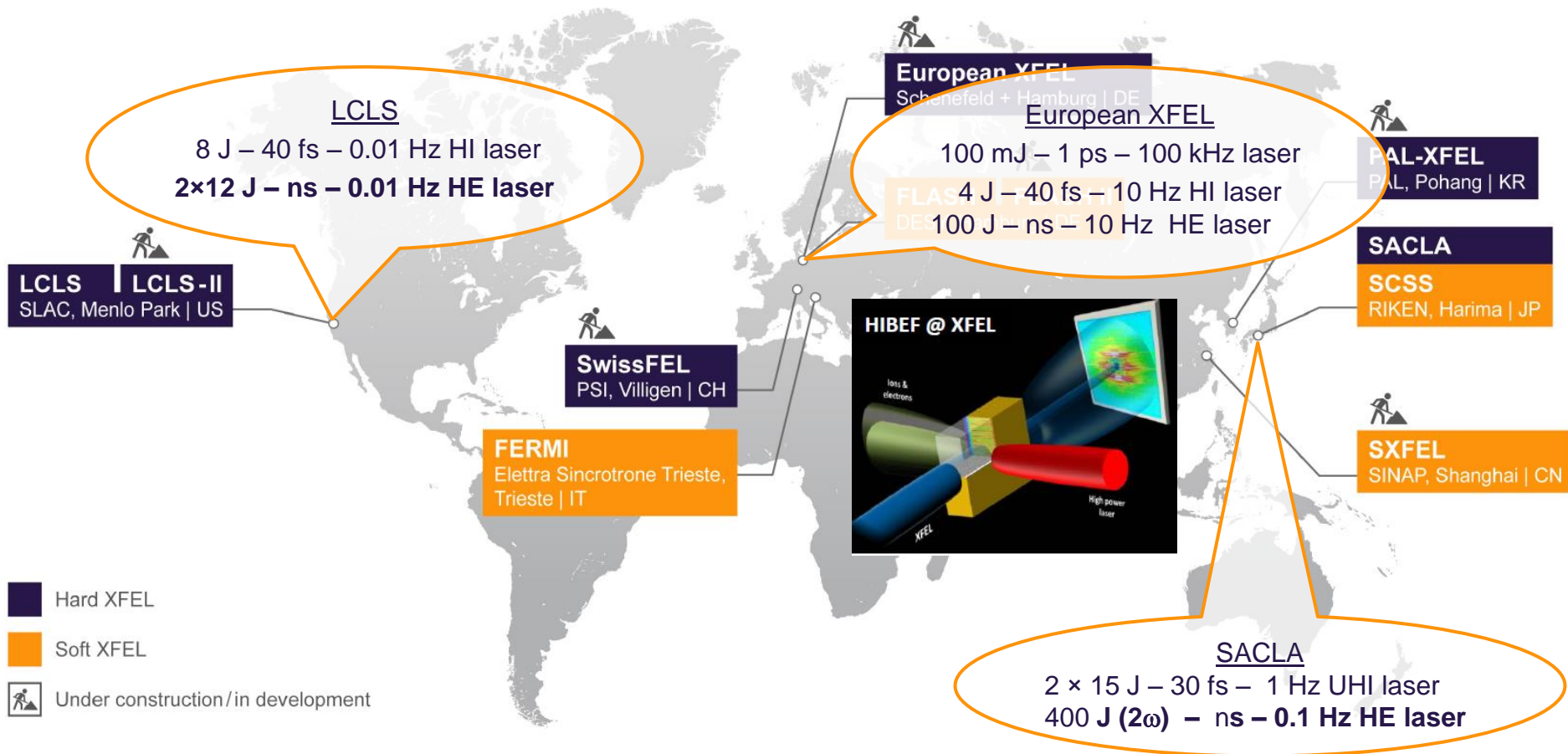
**Jeanloz et al. 2007, Eggert et al. 2008,
Loubeyre et al. 2012, Torchio et al. 2016**

By courtesy of H.-P. Liermann (DESY)



X-ray free-electron lasers worldwide with big OLs

The European XFEL will put Europe in the lead among industrialized nations in a highly competitive scientific and technical environment.



Contents

1. Introduction: Warm Dense Matter

Exoplanets

Planetary Interiors

High-Pressure Experiments

2. DFT-MD Simulations

3. Results

H-He: Jupiter (Saturn)

C-N-O-H: Uranus and Neptune

MgO-FeO-SiO₂: Rocky Planets

4. Outlook

DFT-MD Simulations for WDM

Born-Oppenheimer approximation: combination of (quantum) DFT and (classical) MD

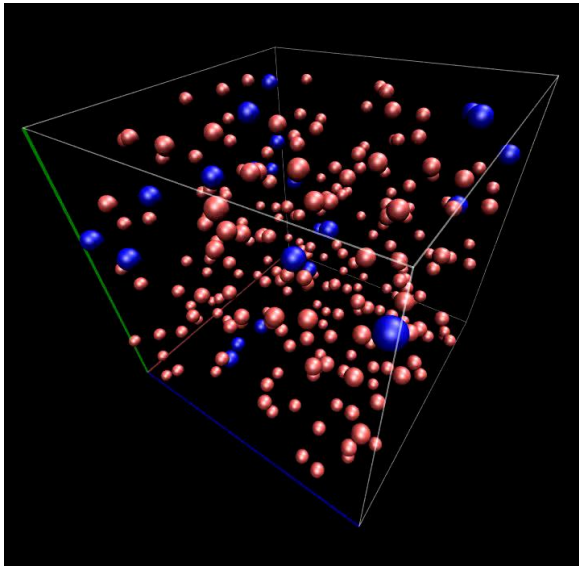
Warm Dense Matter: finite-temperature DFT-MD simulations based on

N.D. Mermin, Phys. Rev. **137**, A1441 (1965)

Codes: **Vienna Ab-initio Simulation Package** (VASP) or Abinit, Quantum Espresso ...

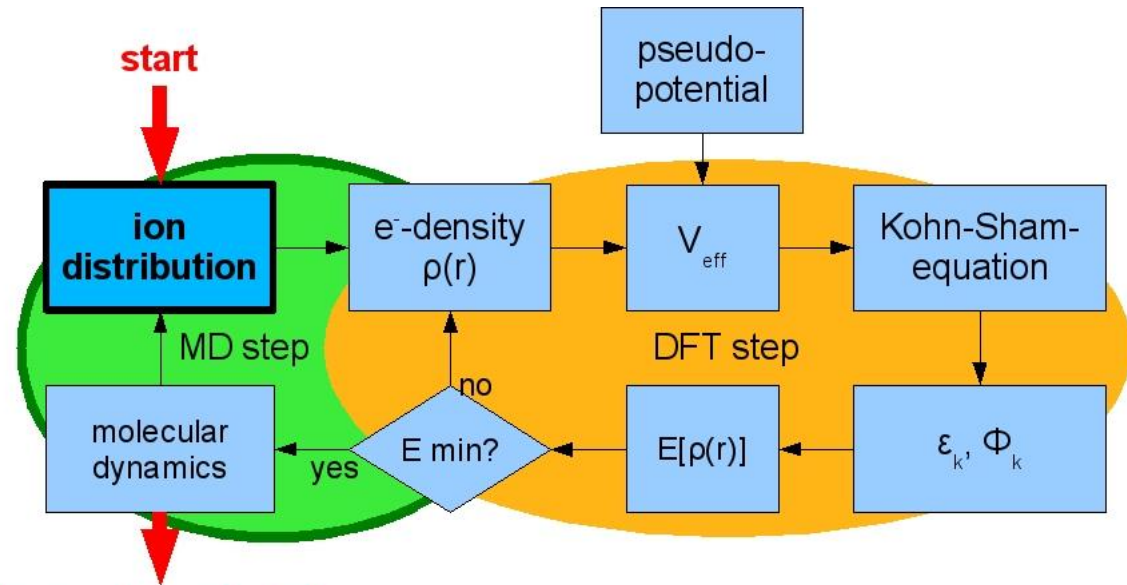
G. Kresse and J. Hafner, PRB **47**, 558 (1993), ibid. **49**, 14251 (1994)

G. Kresse and J. Furthmüller, Comput. Mat. Sci. **6**, 15 (1996), PRB **54**, 11169 (1996)

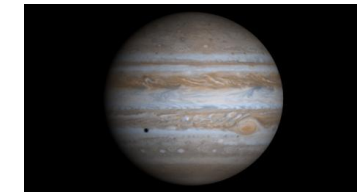


H-He (8.6%) @ 1 Mbar, 4000 K

box length $\sim 10^{-9}$ m

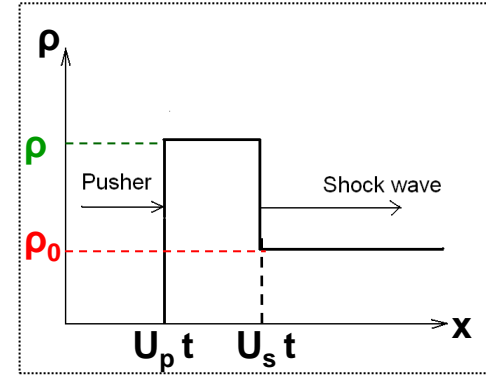
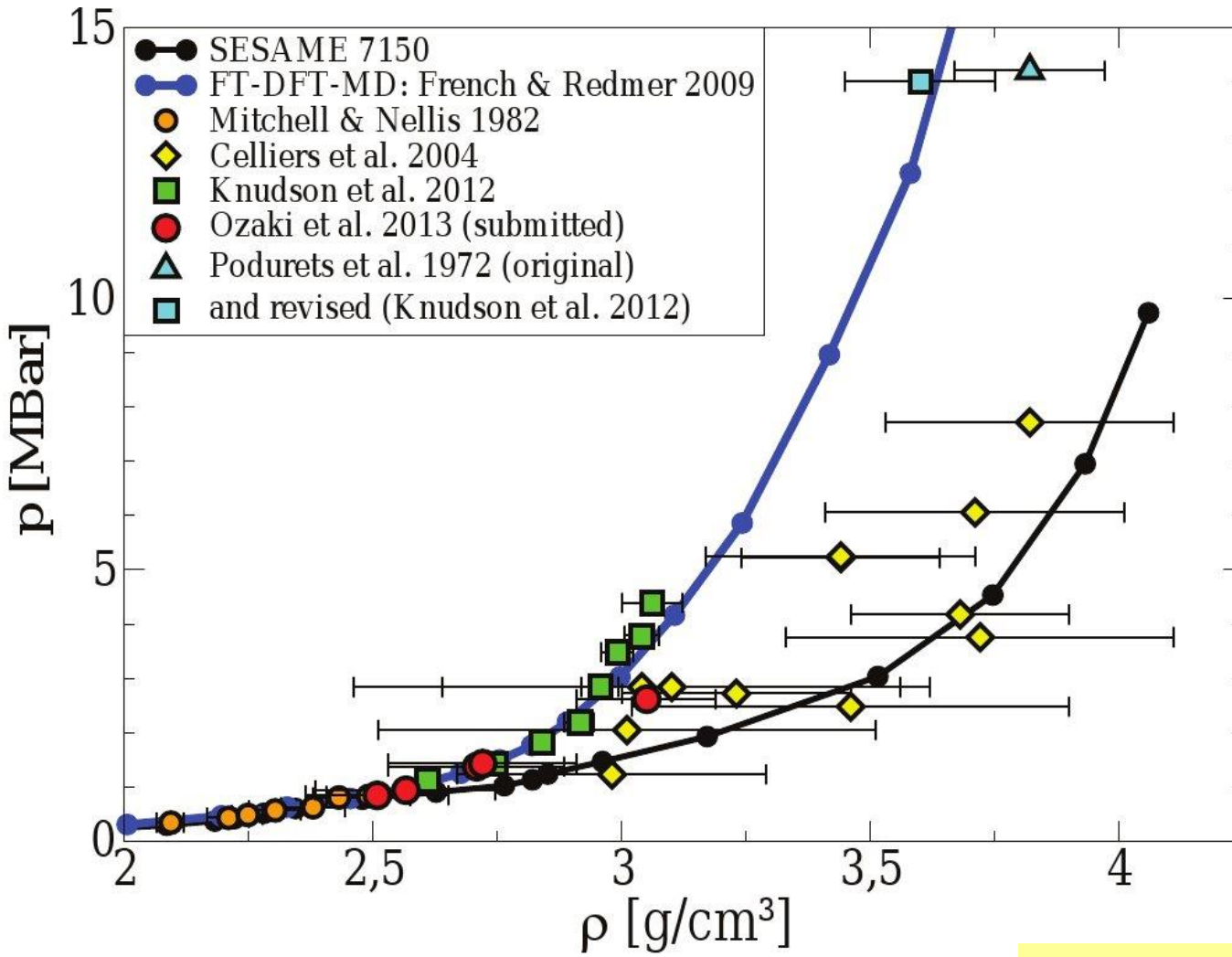


thermodynamic data
high-pressure phase diagram
pair correlation functions
electrical & thermal conductivity
diffusion coefficient
viscosity, opacity

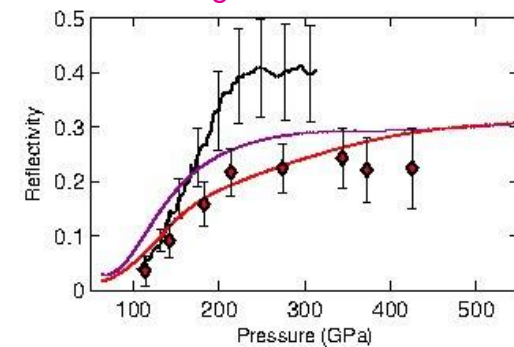


GP size $\sim 10^8$ m

Benchmark: Hugoniot Curve for H₂O



Data:
 Red \diamond \square : Sandia Z
 Open \square : Laser shocks
Theory: FT-DFT-MD
 Red: HSE
 Magenta: PBE



M.D. Knudson et al., PRL 108, 091102 (2012)
 Experiments at Sandia's Z machine

GOOD NEWS:
Very good agreement for EOS and reflectivity (PBE, HSE)

Contents

1. Introduction: Warm Dense Matter

Exoplanets

Planetary Interiors

High-Pressure Experiments

2. DFT-MD Simulations

3. Results

H-He: Jupiter (Saturn)

C-N-O-H: Uranus and Neptune

MgO-FeO-SiO₂: Rocky Planets

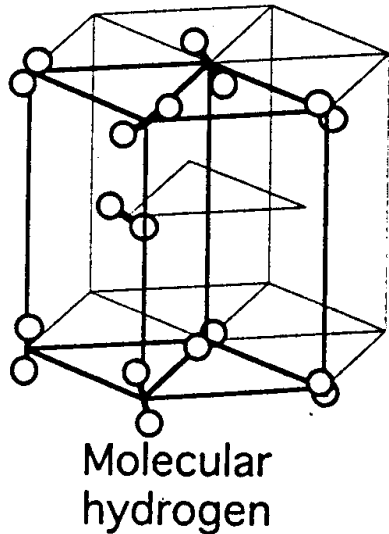
4. Outlook

Solid Metallic Hydrogen at T=0 K?

Proposed by Wigner and Huntington already in 1935 (at 25 GPa).

Verified in recent **DAC** experiments at 5 Mbar?

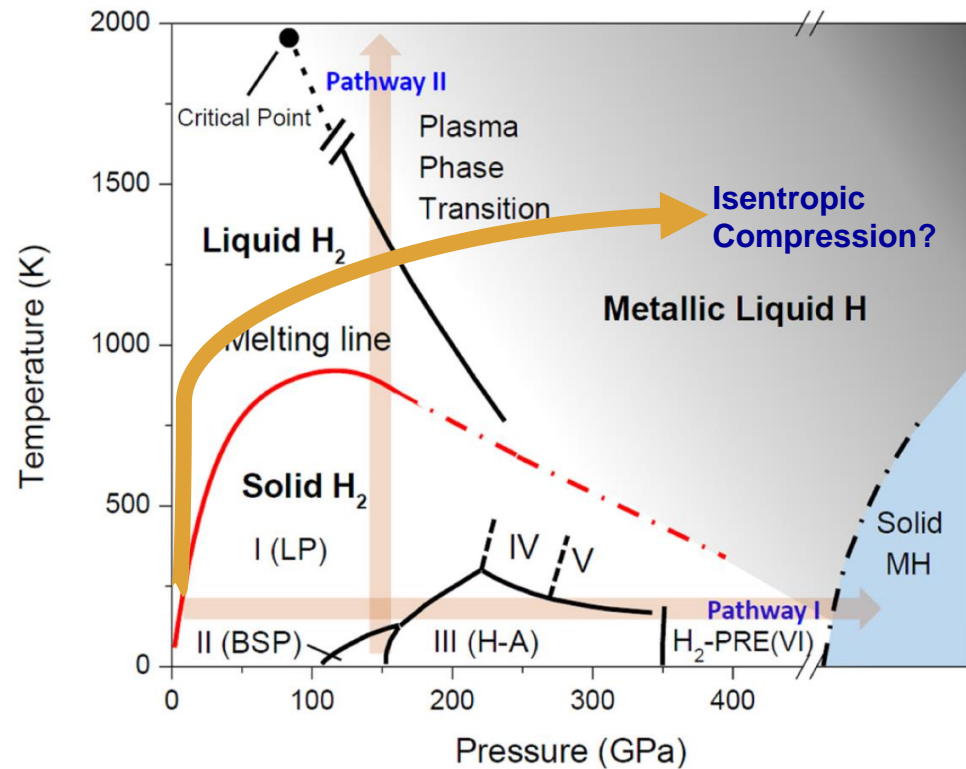
Rich phase diagram obtained in solid H: phases I, II, III, IV, V.



H.K. Mao & R.J. Hemley, RMP **66**, 671 (1994)

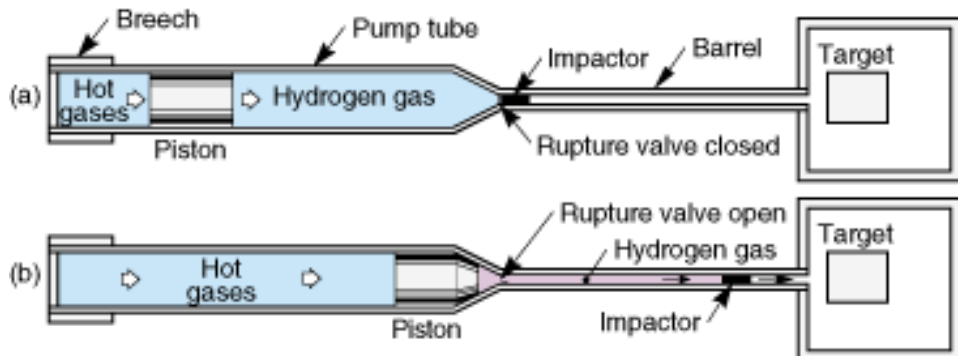
Metallization by band-gap closure:

From 15 eV in the hcp molecular insulator to zero in the bcc metal



R.P. Dias, I.F. Silvera, Science **355**, 715 (2017)
For recent DAC studies, see also:
P. Dalladay-Simpson et al., Nature (2016)
R.S. McWilliams et al., PRL (2016)

Gas Guns: Fluid Metallic Hydrogen



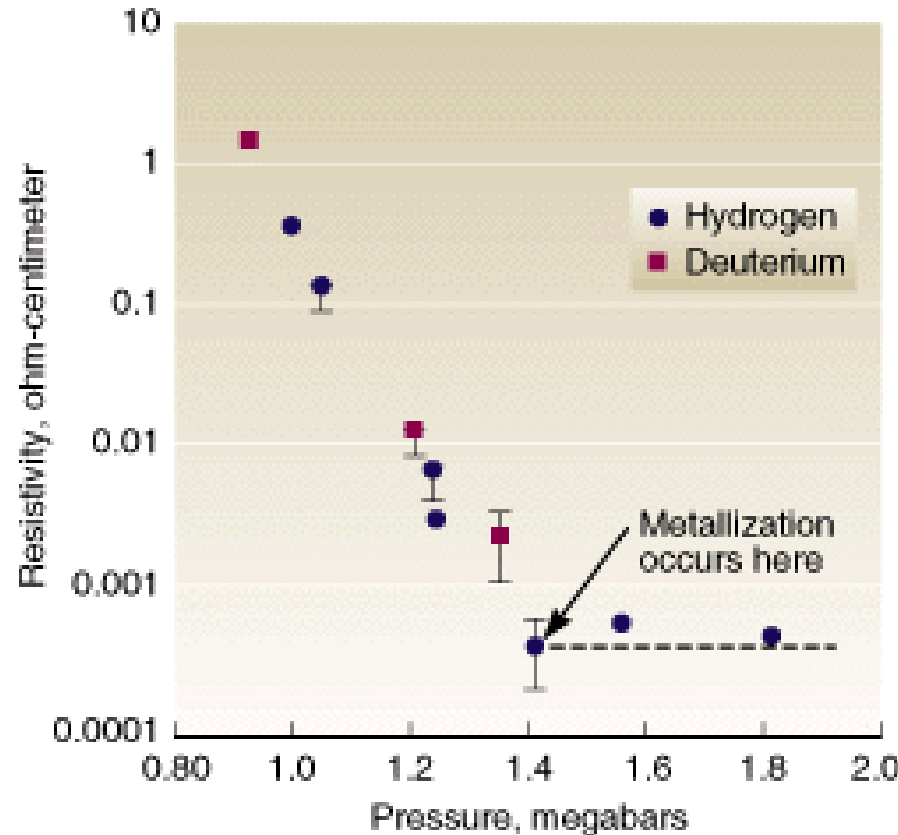
(a) In the first stage of the gas gun (blue shading), hot-burning gases from gunpowder drive a piston, which in turn compresses hydrogen gas. (b) In the second stage (pink shading), the high-pressure gas eventually ruptures a second-stage valve, accelerating the impactor down the barrel toward its target.

Reverberating shock waves in sandwich target

- quasi-isentropic process
- „low“ temperatures

Metallic conductivity observed at ~3000 K and 1.4 Mbar

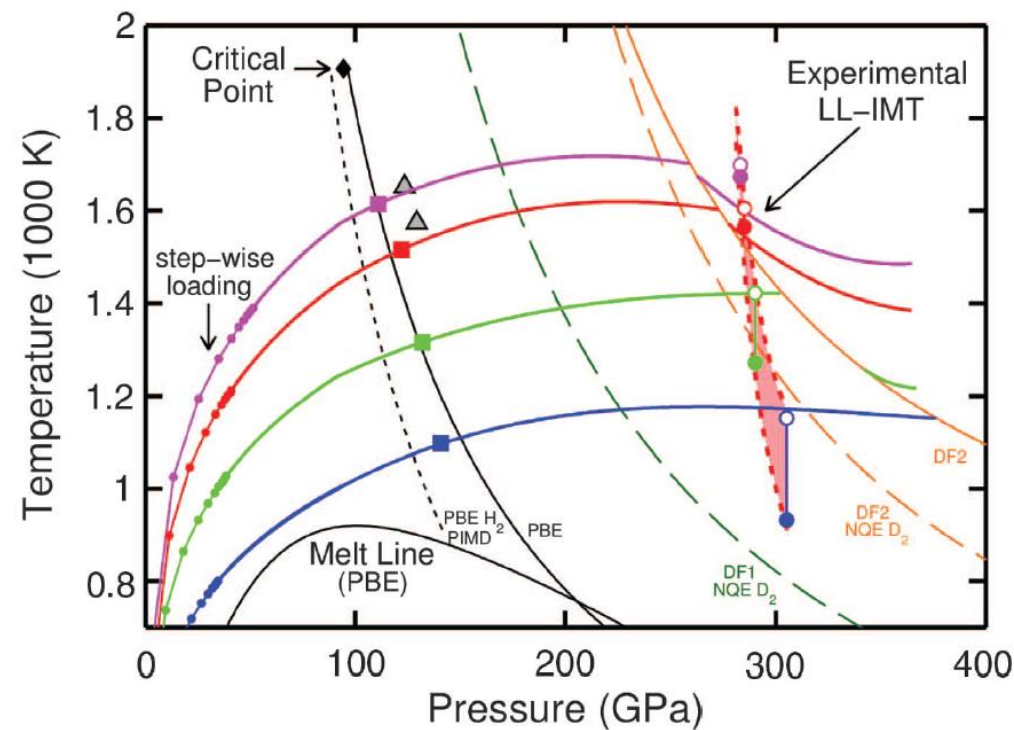
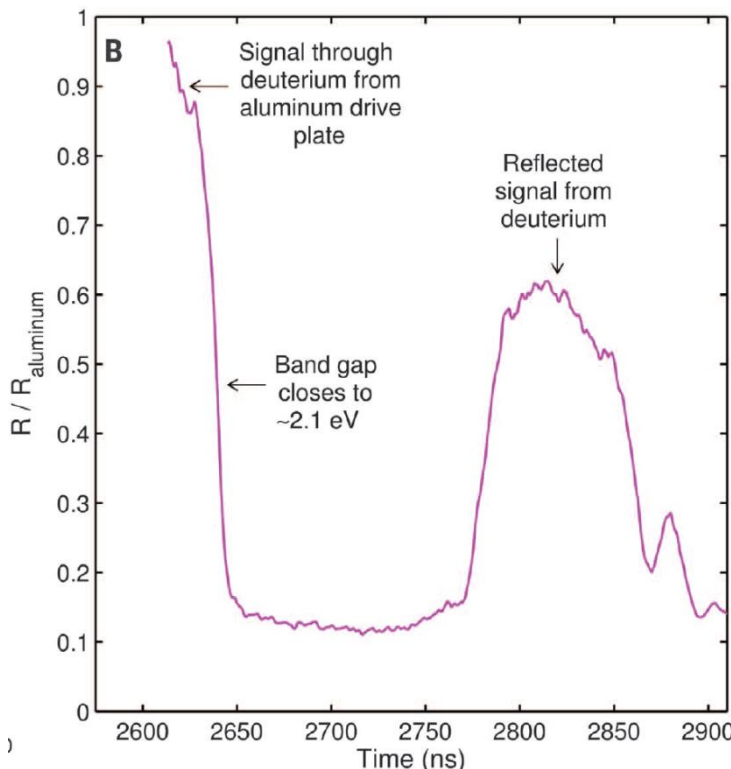
W.J. Nellis et al., PRL 68, 2937 (1992)
S.T. Weir et al., PRL 76, 1860 (1996)



But no indication of a first-order phase transition!

Abrupt Insulator-to-Metal Transition - Typical of a first-order LL-PT

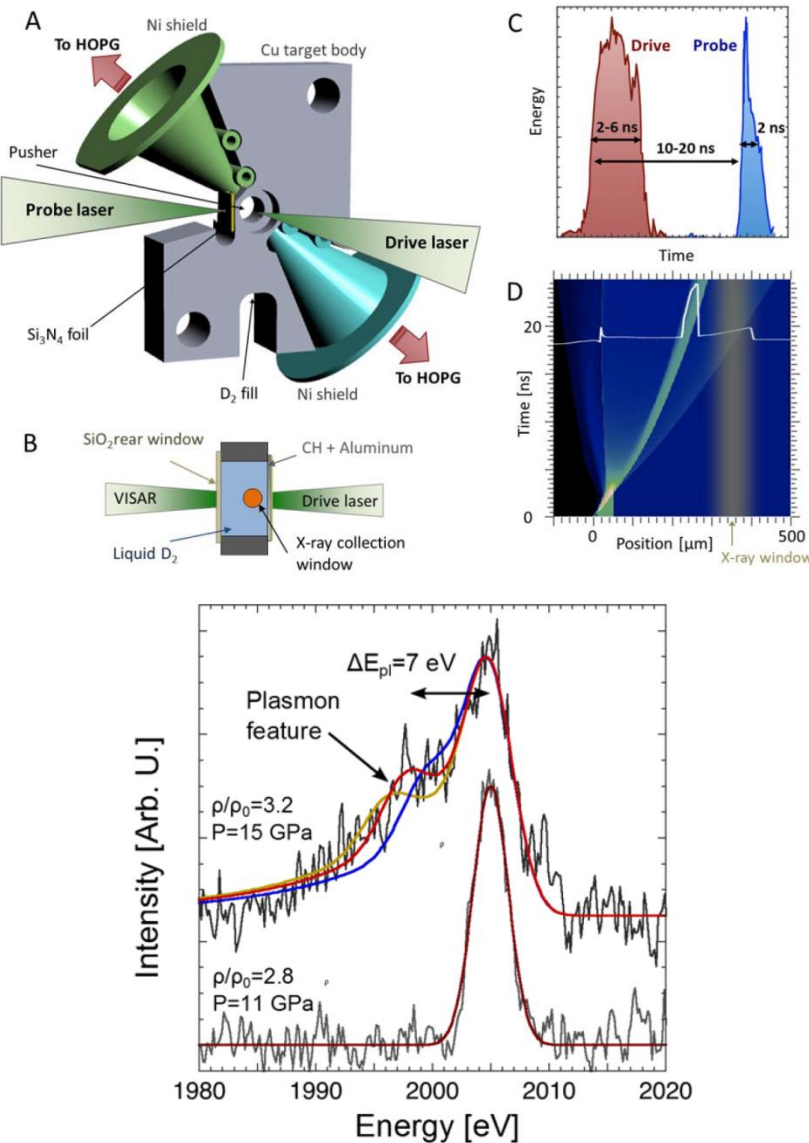
M.D. Knudson, M.P. Desjarlais, A. Becker, R.W. Lemke, K.A. Cochrane, M.E. Savage, D.E. Bliss, T.R. Mattsson, RR, Science 348, 1455 (2015)



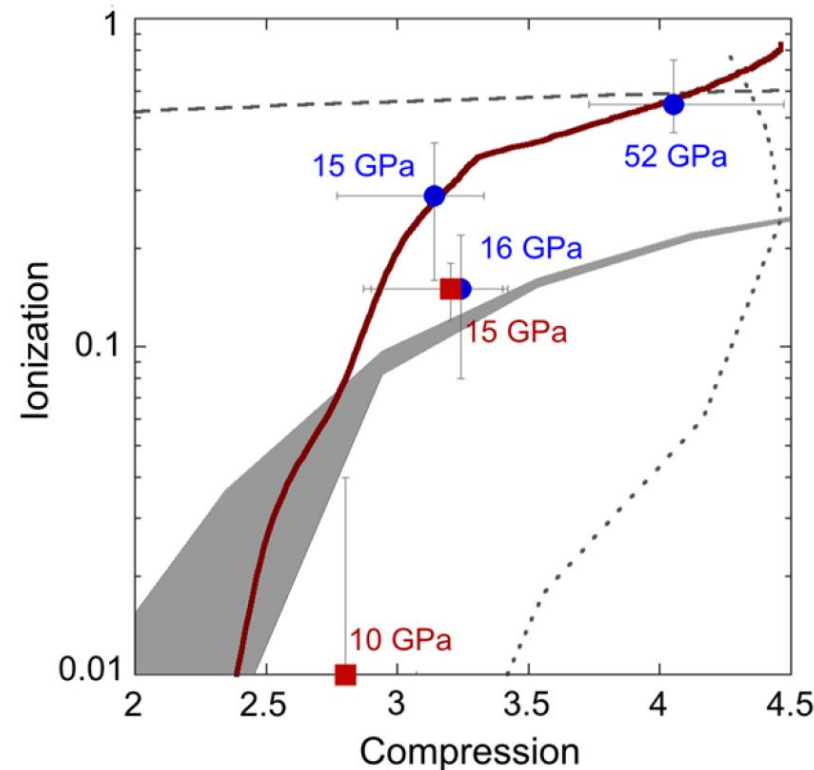
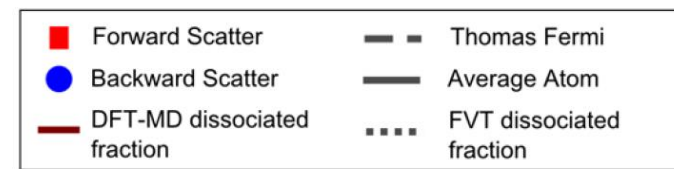
Measure the shock compression path and reflectivity, check with DFT-MD (Z Fundamental Science Program).

LL-IMT at ~3 Mbar below 2000 K:
Indication of a first-order LL-PT.

X-ray Thomson Scattering Probes Onset of Dissociation in Jupiter



P. Davis et al., Nature Commun. **7**, 11189 (2016)
 Experiment: Janus Laser Facility (LLNL)
 DFT-MD: A. Becker (U Rostock)



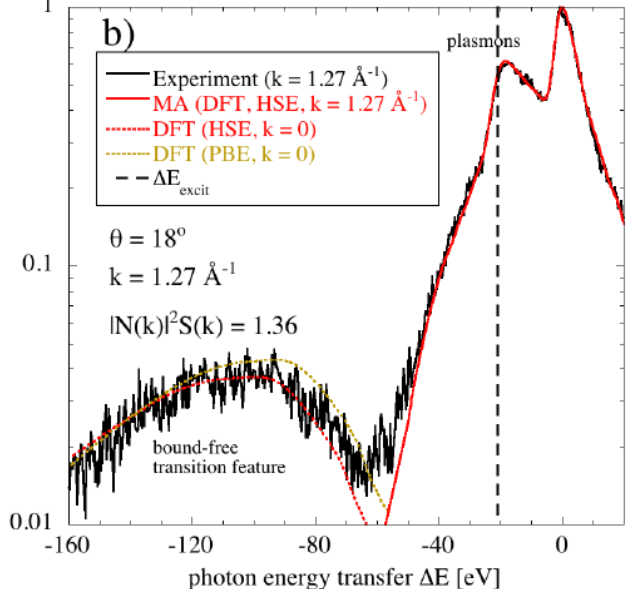
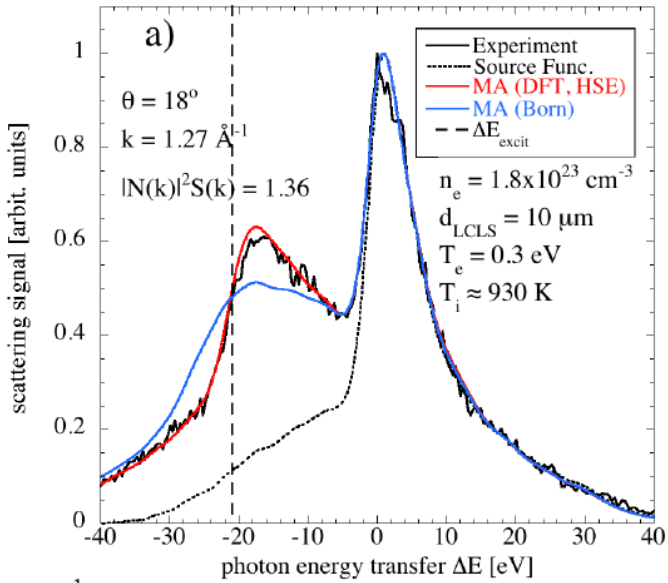
XRTS Experiments at FELs: LCLS

P. Sperling et al., PRL 115, 115001 (2015)

B. Witte et al., PRL 118, 225001 (2017)

BMA

DFT-MD



AI

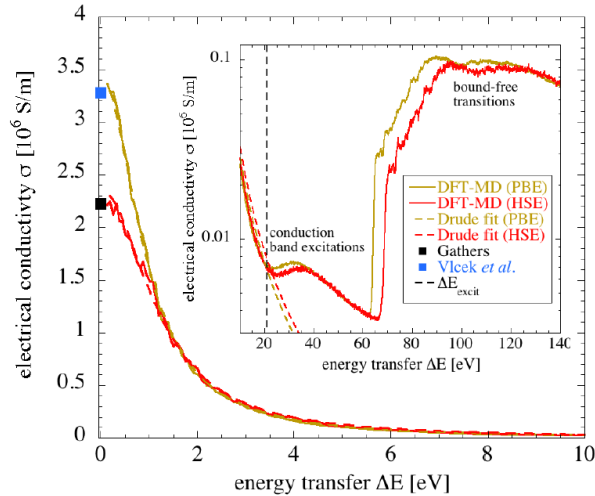
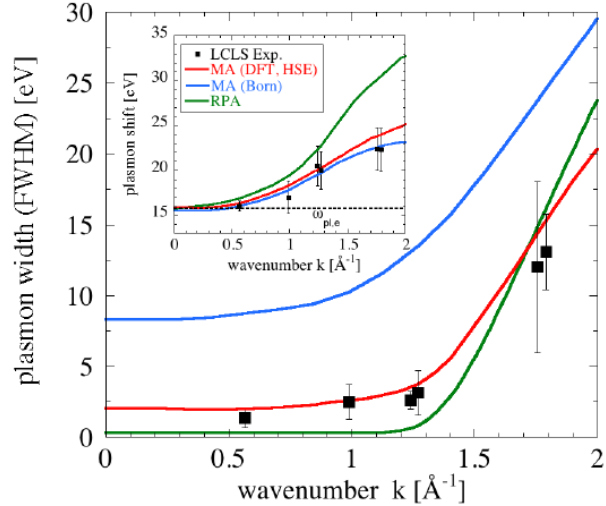
Full XRTS spectrum calculated with DFT-MD simulations:

1. Excellent agreement with high-resolution LCLS experiments.

2. Plasmon dispersion (shift and width) in agreement with experiment.

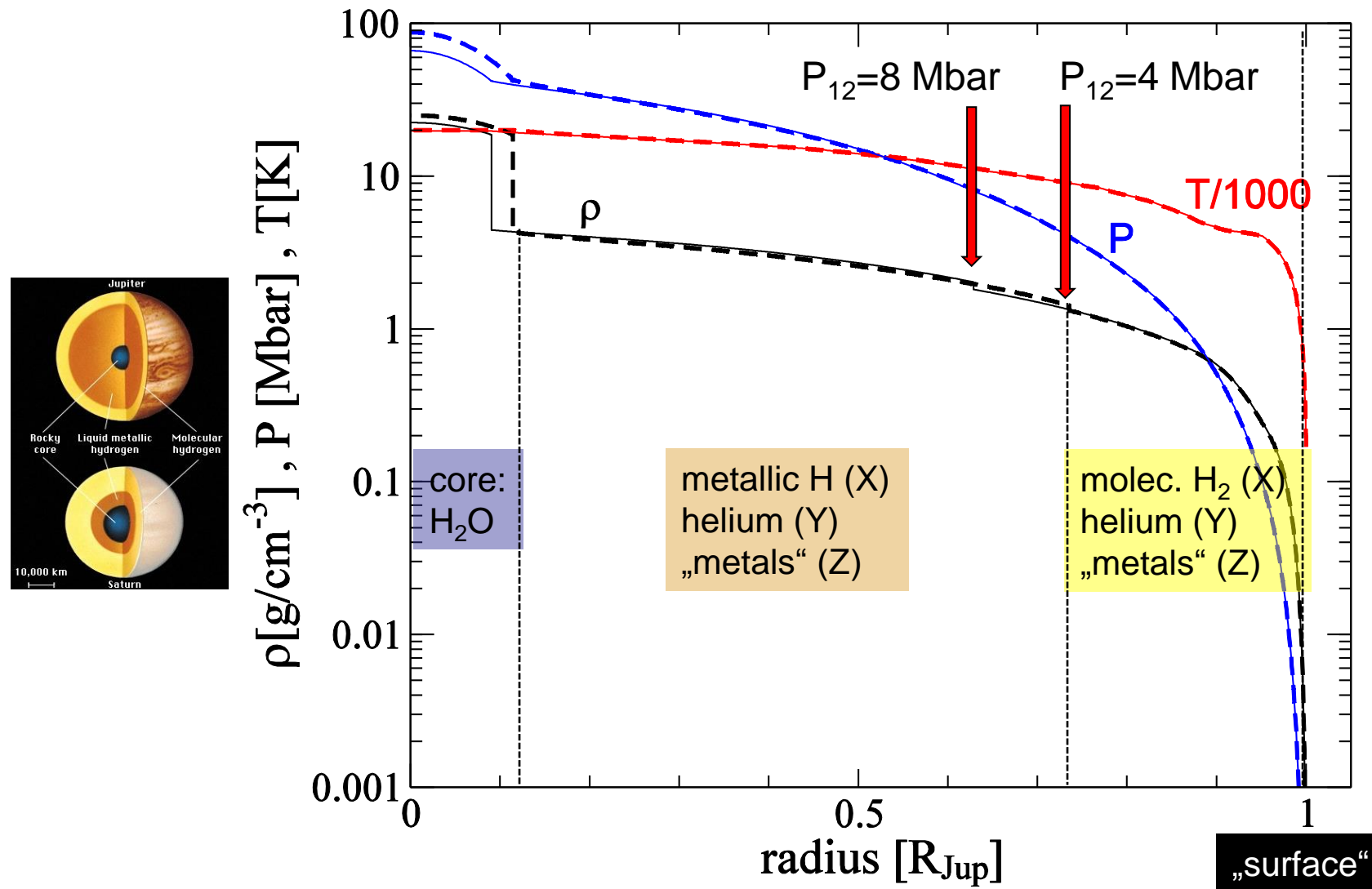
3. HSE superior to PBE XC functional in the DFT calculations.

4. Non-Drude electrical conductivity derived from f-f transitions (Cooper minimum).



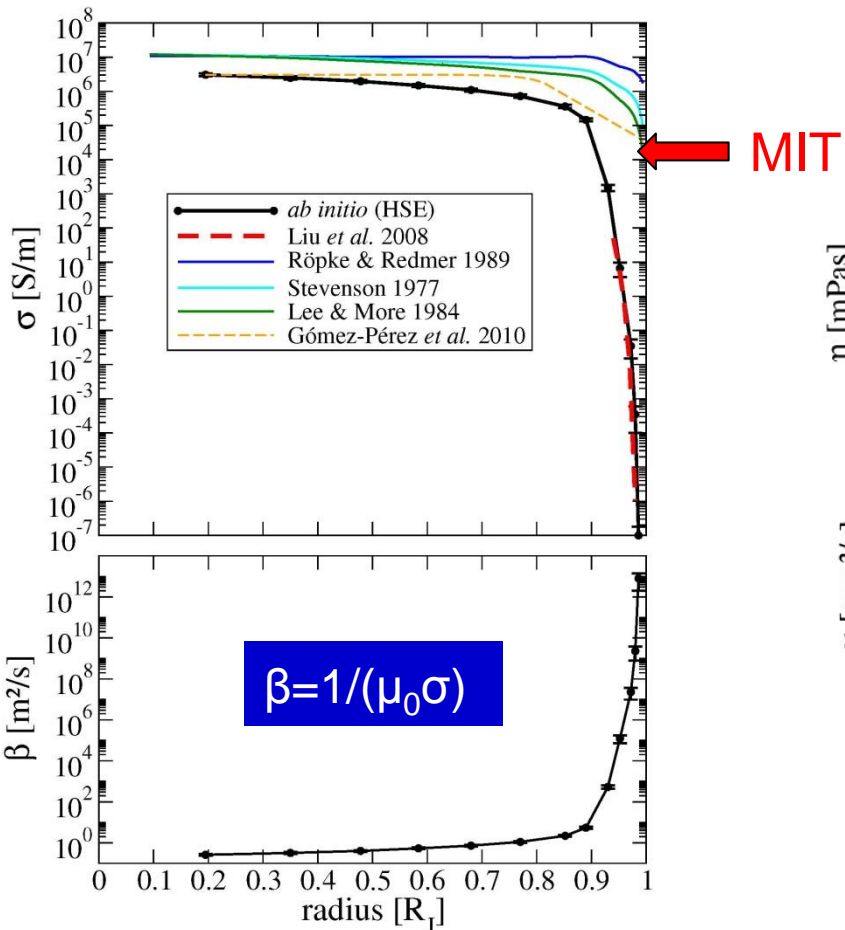
Jupiter's Interior with LM-REOS (H-He-H₂O)

Assuming a three-layer structure

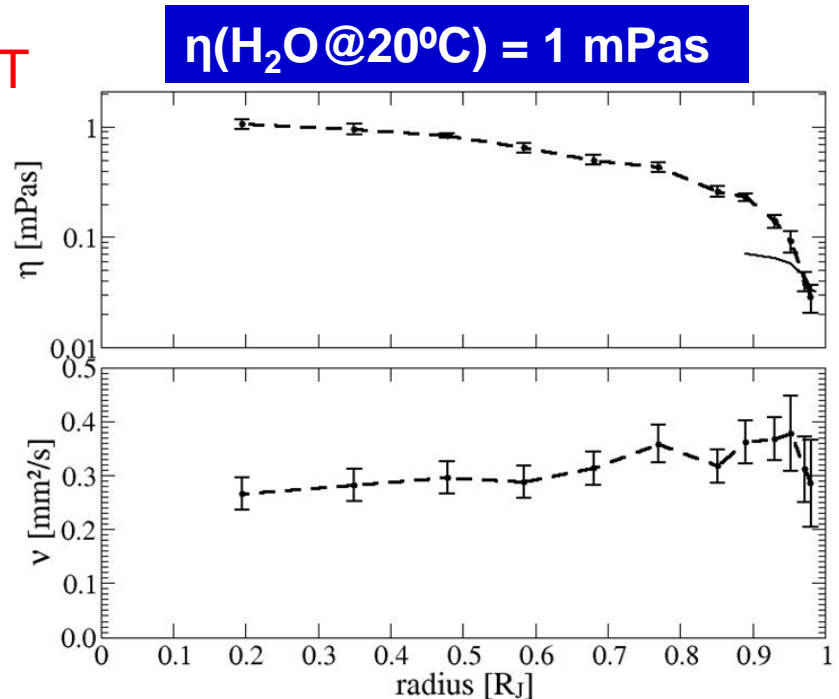


Material Properties along Jupiter's Isentrope

M. French et al., ApJS 202, 5 (2012): self-consistent EOS and material data from DFT-MD.
Used for planetary modeling (interior, dynamo, evolution)



Electrical conductivity σ and magnetic diffusivity along Jupiter's isentrope.

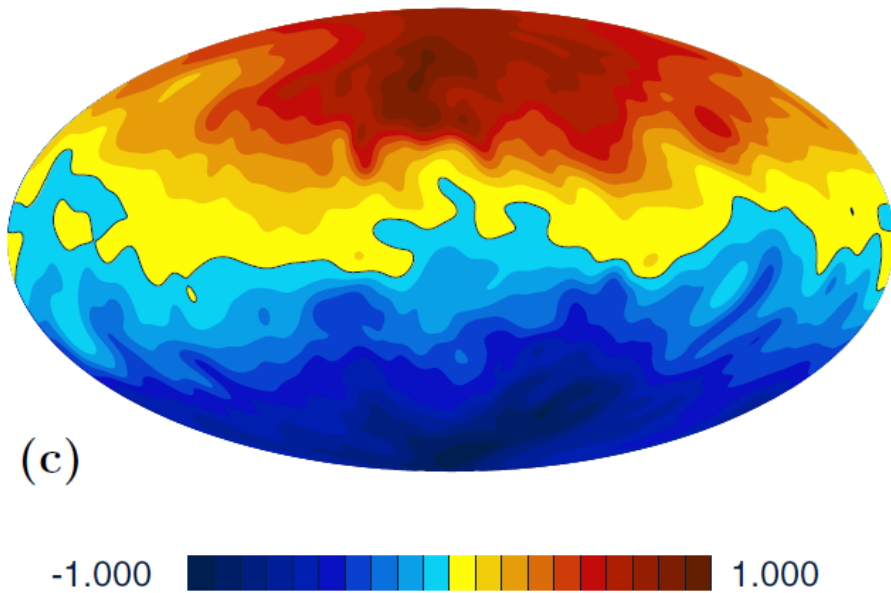


Dynamic (η) and kinematic ($\nu = \eta/\rho$) viscosity along Jupiter's isentrope.

$$\eta = \frac{\Omega}{3k_B T} \int_0^\infty dt \sum_{ij=\{xy,yz,zx\}} \langle p_{ij}(0)p_{ij}(t) \rangle$$

Jupiter's Magnetic Field

Dynamo simulations based on self-consistent EOS and material data from DFT-MD:
M. French et al., ApJS 202, 5 (2012)



Snapshot of the radial component of the dipolar magnetic field of Jupiter.

C. Jones, Icarus 241, 148 (2014)

DFG SPP 1488 Planetary Magnetism (2011-2016):

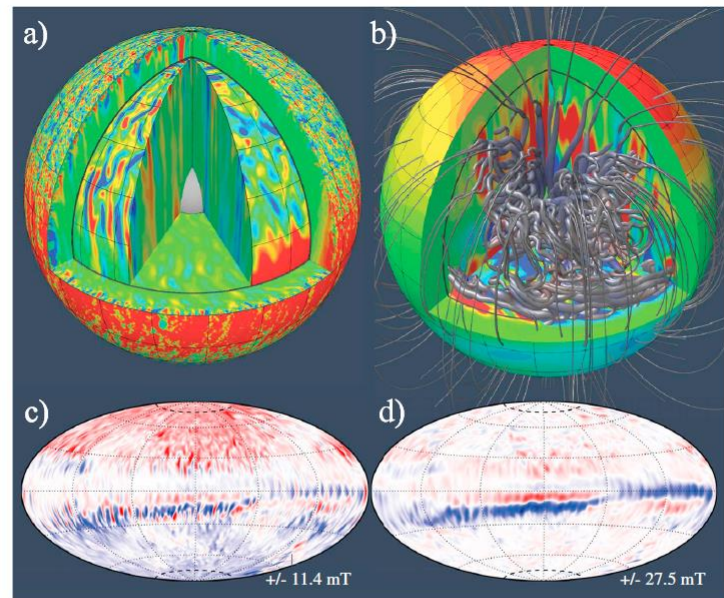


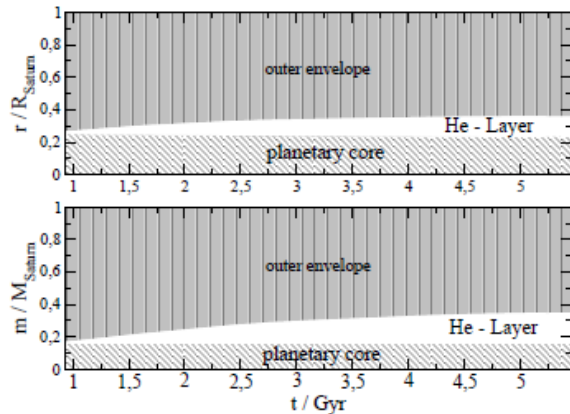
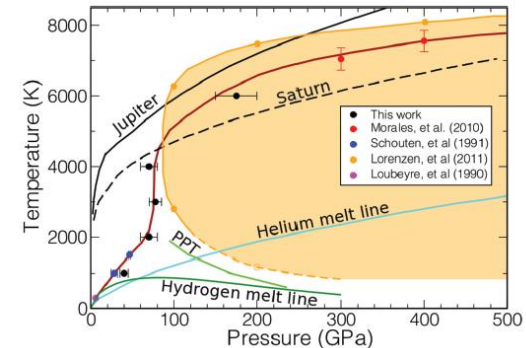
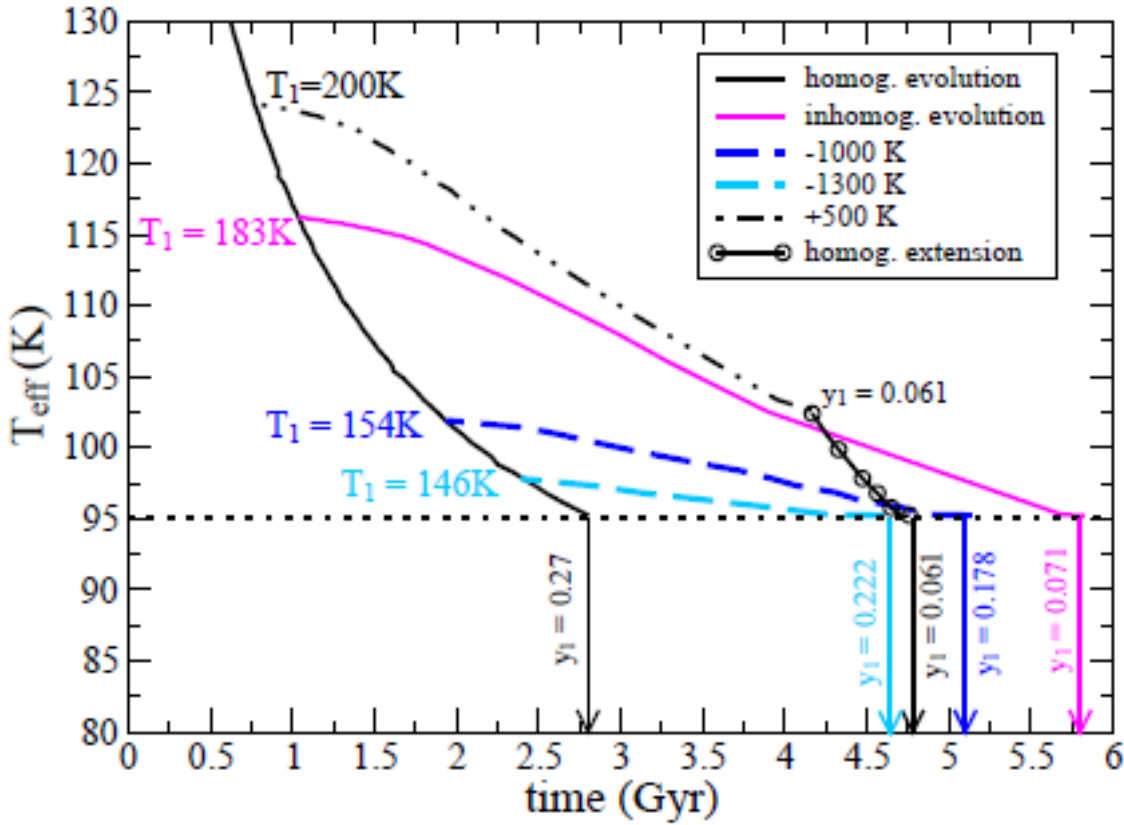
Figure 2. (a) The azimuthal flow component on the outer surface and the right cut, and the radial flow component in the equatorial and left cuts. The inset sphere slices visualize the weaker flow at greater depths. The right inset shows the azimuthal flow amplified by a factor of 10, and the left inset shows the radial flow amplified by a factor of 2.5. The flow amplitude strongly increases with radius, while the length scale decreases. (b) The radial magnetic field on the outer surface and the left cut. The surface field has been amplified by a factor of 10. The right and horizontal cuts (at -10°) show the azimuthal magnetic field. The thickness of the magnetic field lines has been scaled with the third root of the local magnetic field strength. (c and d) The radial and azimuthal magnetic fields at the transition radius $0.87 r_0$ that is marked with a dark grey line in Figures 2a and 2b. Yellow/red (blue) indicates outward (inward) or eastward (westward) directions.

T. Gastine et al., GRL 41, 5410 (2014)

Saturn Cooling Curves using the 2009 Lorenzen et al. H-He Phase Diagram

Lorenzen H-He EOS with demixing available for all He concentrations.

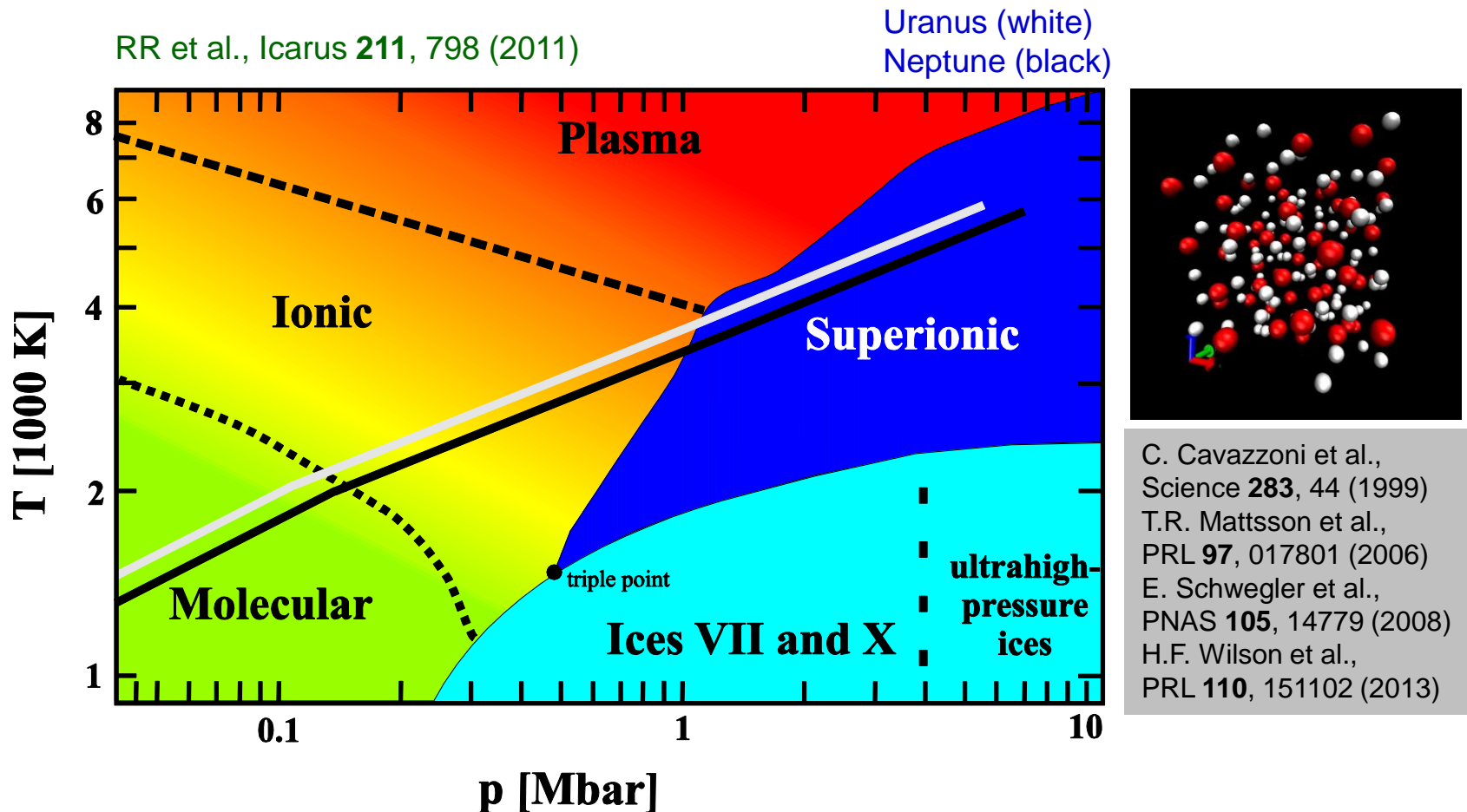
Shifts by $\Delta T = -1300$ K and $\Delta T = +500$ K yield the correct cooling time.



R. Püstow, N. Nettelmann, W. Lorenzen, RR, Icarus **267**, 323 (2016).

New calculations based on vdW-DF H-He EOS for interior and evolution are on the way.

Ice Giants – High Pressure Phase Diagram for C-N-O-H: H₂O



EOS and phase diagram:

M. French et al., PRB **79**, 054107 (2009)

Transport properties (diffusion, conductivity):

M. French et al., PRB **82**, 174108 (2010)

Water ices VII and X:

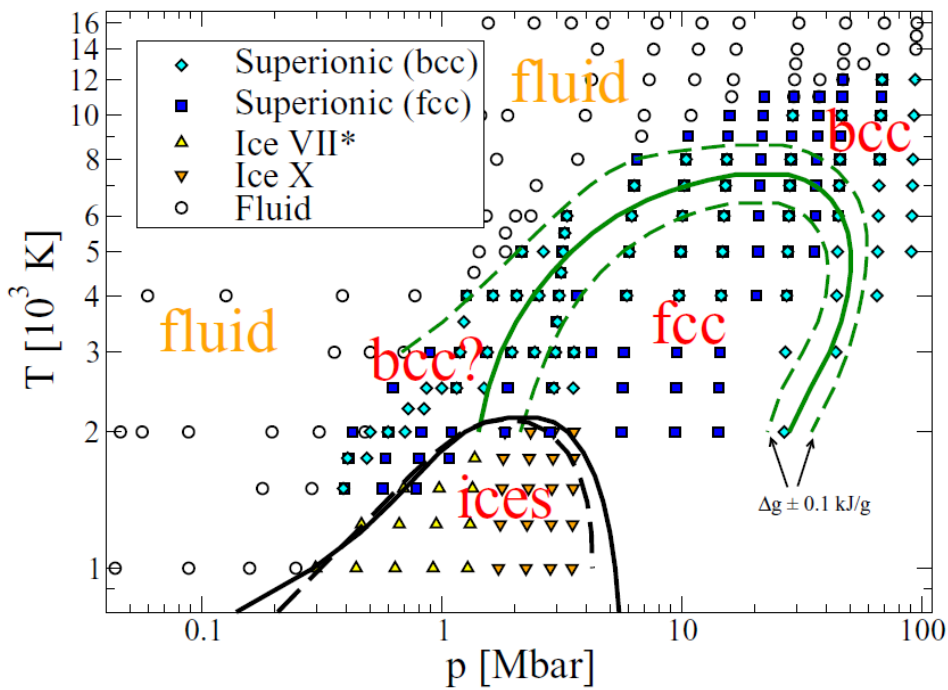
M. French, RR, PRB **91**, 014308 (2015)

Superionic bcc and fcc phases:

M. French et al., PRB **93**, 022140 (2016)

H_2O : Superionic Phases and Conductivity

Dynamo (deep interior) and Ohmic dissipation (atmosphere)



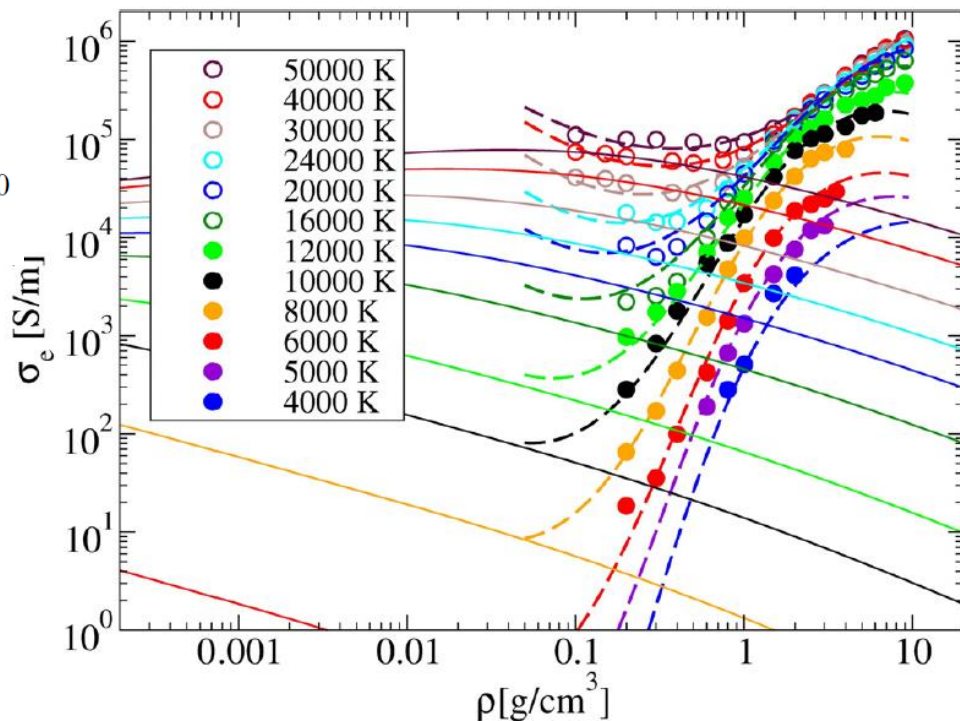
M. French, RR, PRE **93**, 022140 (2016)

Free energy functional for the EOS of ice VII and X.

Small differences between EOS data for fcc and bcc SI.

DFT data from Kubo-Greenwood formula.
Dashed lines: fit function.
Solid lines: multi-component conductivity model for low-density fluid.

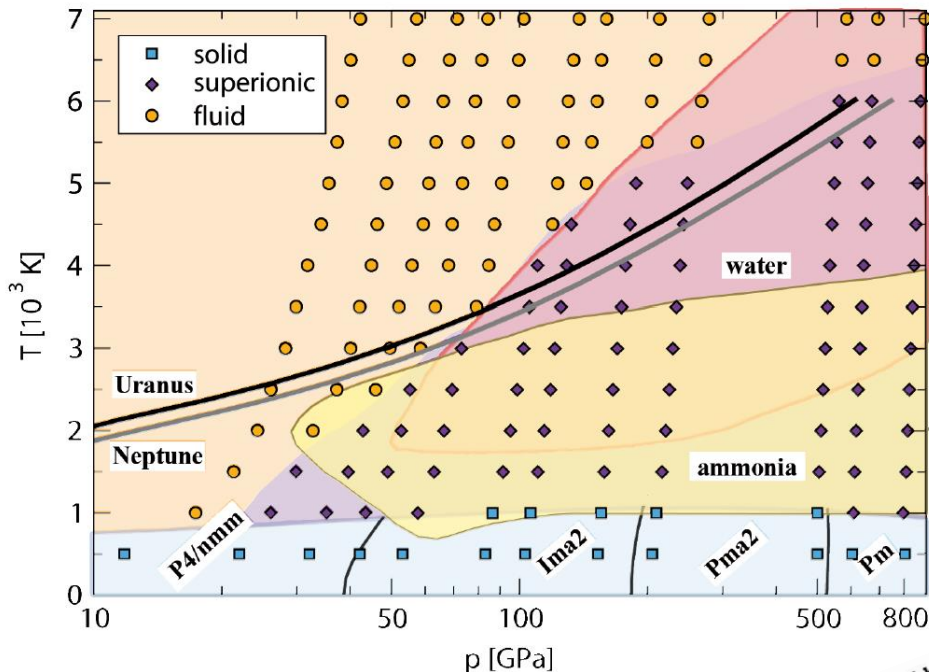
M. French, RR, PoP **24**, 092306 (2017)



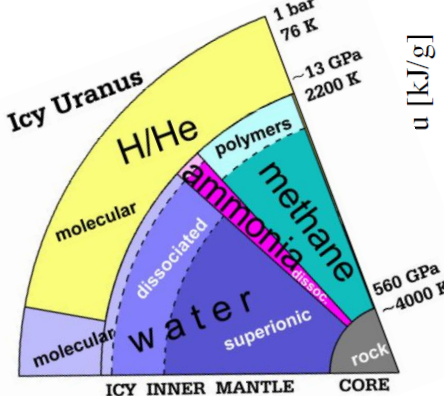
Uranus and Neptune: C-N-O-H

$\text{H}_2\text{O:NH}_3 = 1:1$ mixture:

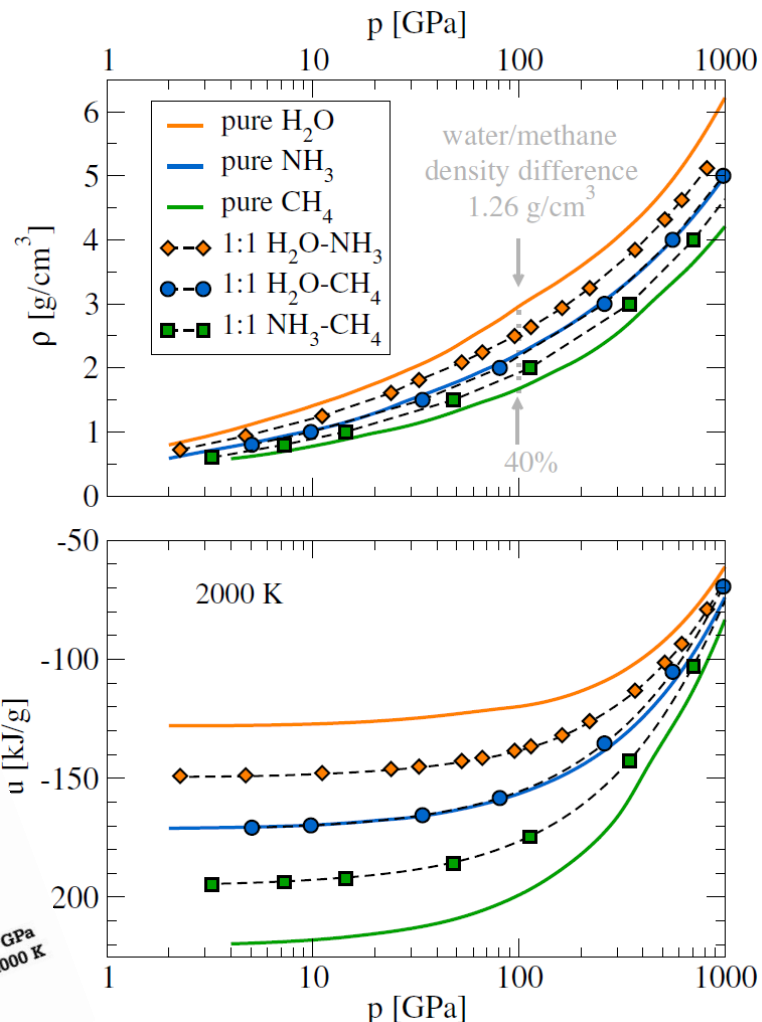
Superionic phase occurs as in H_2O , NH_3 !



M. Bethkenhagen et al.,
JPCA **199**, 10582 (2016)



Validity of linear mixing for C-N-O-H:
Amagat's law works well!



M. Bethkenhagen et al., ApJ **848**, 67 (2017)

Neptune-sized Exoplanet GJ 436b

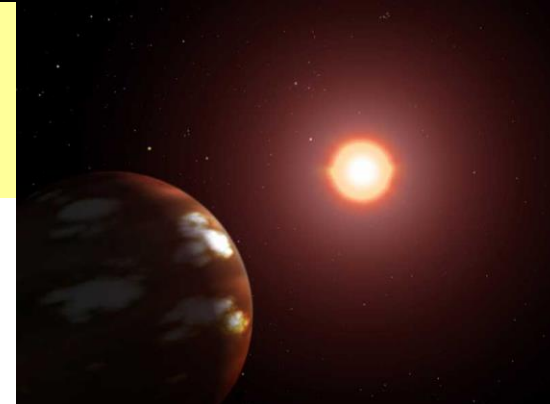
Mass-radius relation for transiting planets known (plus radial velocity method)

	Neptune	GJ 436b
mass [M_{\oplus}]	17.13	22.2 ± 1
radius [R_{\oplus}]	3.86	4.327 ± 0.183
surface temperatur [K]	70 (at 1 bar)	712 ± 36
semi major axis [AU]	30	0.0291 ± 0.0004
period	165 years	2.6439 days

Host star is M Dwarf with $T_{\text{eff}}=3350$ K and
 $M=0.44 M_{\text{Sun}}$, 33 Ly away (Leo)
H.L. Maness et al., PASP **119**, 90 (2007)

Observational parameters:

M. Gillon et al., A&A **471**, L51 (2007),
B.-O. Demory et al., A&A **475**, 1125 (2007)

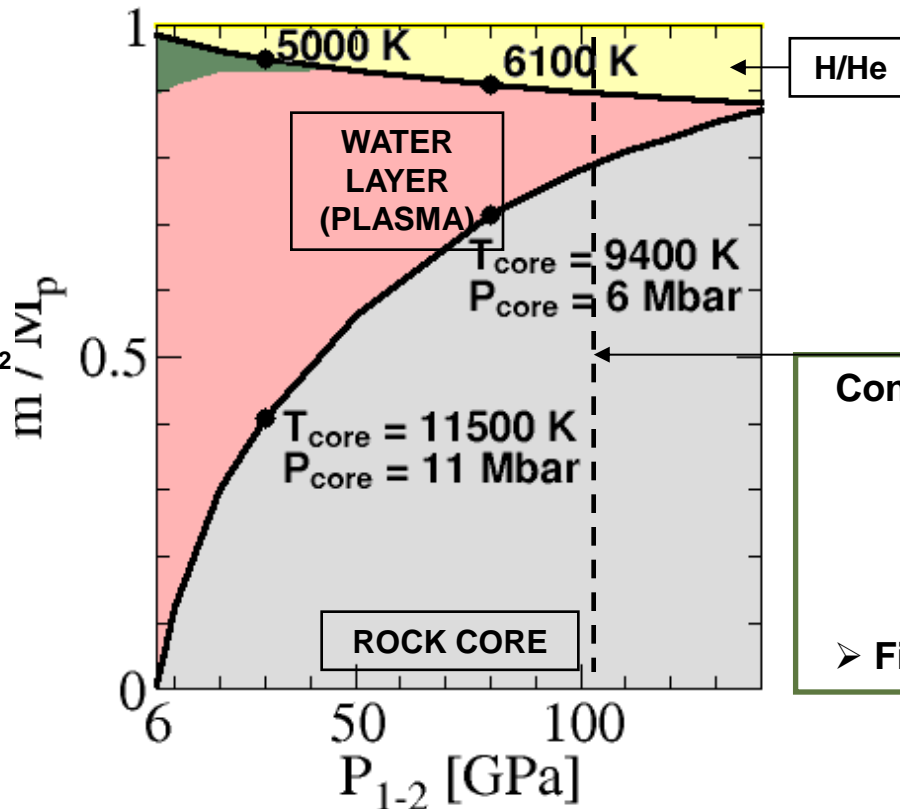
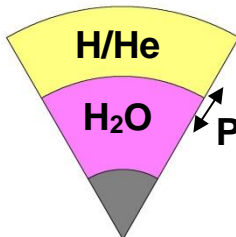


GJ 436b: Neptune-like or Super-Earth?

J. Wright: exoplanets.eu (2007)

Structure calculations limit the H/He mass fraction down to 1 - 12% M_p .

Illustration



Constraints from formation:

$H/H=10-20\%$

$ice=17-40\%$

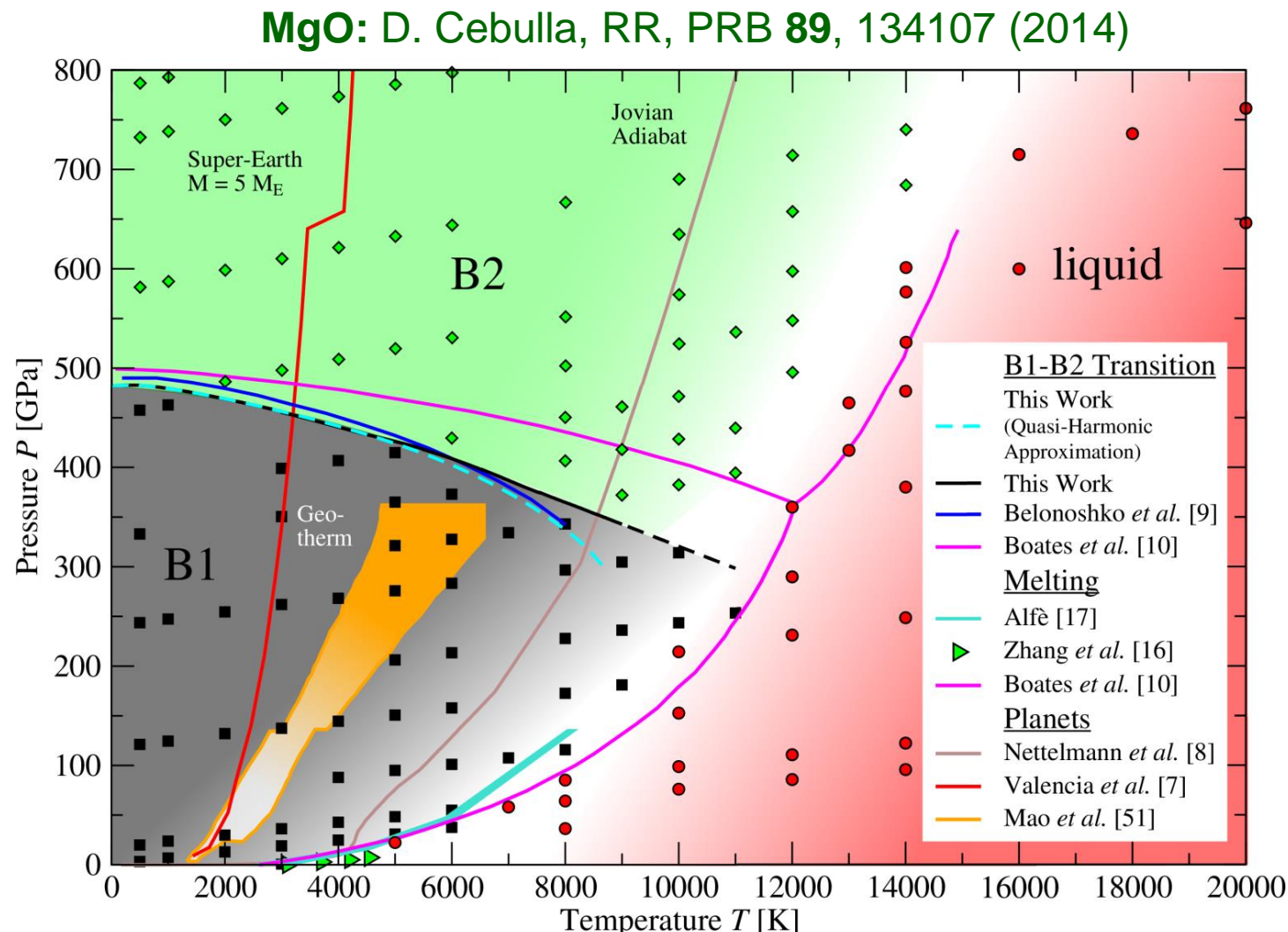
$rock=45-70\%$

➤ Figueira et al., A&A (2009)

CONCLUSION: Models with $M_{core} \sim 0.7 M_p$ are consistent with all constraints.

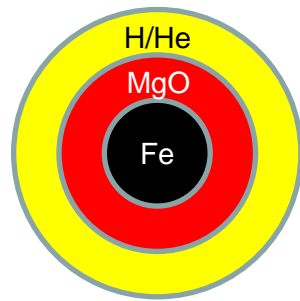
N. Nettelmann et al., A&A 523, A26 (2010)

High Pressure Phase Diagram for MgO-FeO-SiO₂ – Earth, super-Earths



Dynamic compression experiments:
McWilliams *et al.* (2012), Coppari *et al.* (2013), Root *et al.* (2015).

M-R Relation and Interior Models for Super-Earth Kepler 10b



G star 560 Ly away

Kepler 10b:

$R \sim 1.475 R_E$

$M \sim 4.6 M_E$

$a = 0.01864$ AU

$T = 0.8375$ d

Kepler 10c:

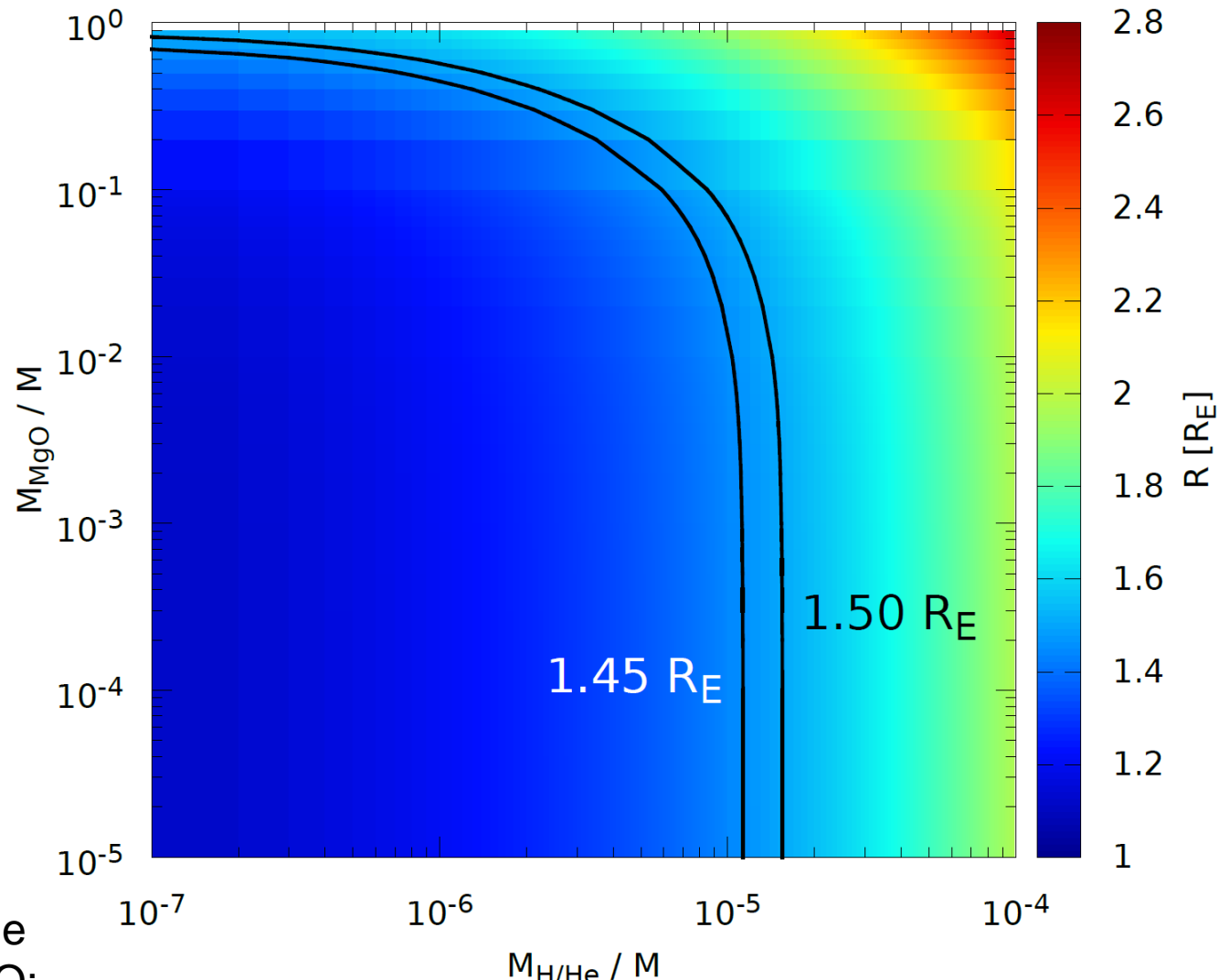
$R \sim 2.35 R_E$

$M \sim 17.2 M_E$

$a = 0.241$ AU

$T = 45.3$ d

Solutions depend on the structure assumed and the EOS used (H/He and MgO:
DFT-MD)



Discovery Science proposal: 3 NIF shot days granted - D_WDM_XRTS_Be 2017/11/07-08

SLAC

Proposal for NIF facility time

Collisions and conductivity of matter at the extreme densities and temperatures found in brown dwarfs

Proposal category: Data acquisition

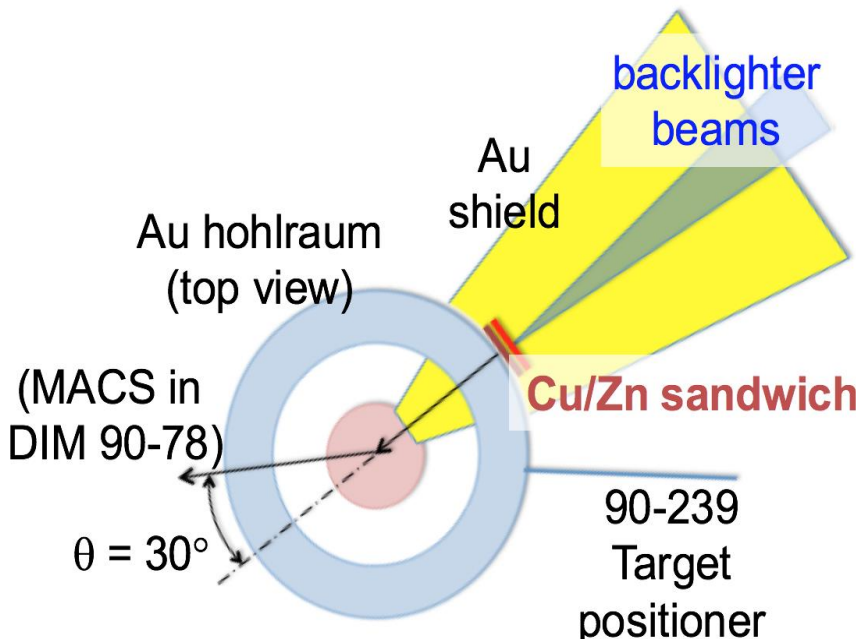
Principal Investigator: Ronald Redmer,

Facility POC: T. Doeppner, LLNL

Team:

Name	Institution	role/ tasks
Ronald Redmer	Rostock University	PI, DFT-MD simulations
Bastian Witte	Rostock University	DFT-MD simulations and conductivity calculations
Siegfried Glenzer	SLAC	experimental design
Luke Fletcher	SLAC	experimental design, data analysis
Eliseo Gamboa	SLAC	experimental design, data analysis
Philipp Sperling	XFEL, DESY, Germany	Hydro-dynamic and DFT-MD simulations
Carsten Fortmann	XFEL, DESY, Germany	X-ray Thomson scattering simulations
Paul Neumayer	GSI, Germany	experimental design, data analysis
Sven Toleikis	DESY, Germany	experimental design
Laurent Divol	LLNL	drive design and post-shot modeling
Tilo Doeppner	LLNL	Co-I, Liason, experimental design, execution
Otto Landen	LLNL	experimental design
John Kline	LANL	Be drive design
Austin Yi	LANL	Be drive design

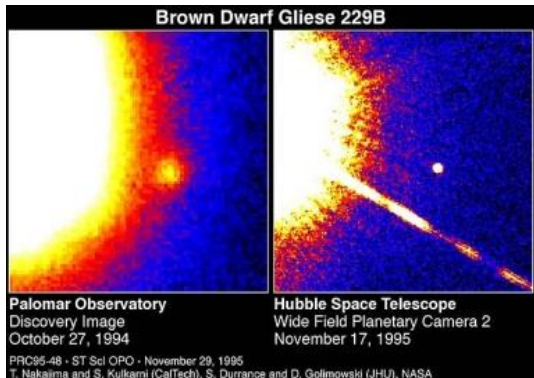
Collective XRTS with Be at 40 g/cm³



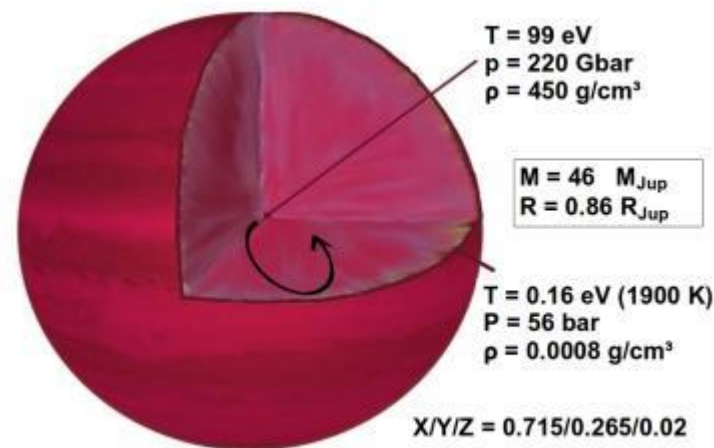
- Number of beams: 192
- Total energy: ≤ 0.9 MJ
- Total peak power: 200TW
- per beam: < 1.1 TW
(except backlighter beams)

Physics of Brown Dwarfs

- Jupiter-sized: $13 M_{Jup} < M < 75 M_{Jup}$
- Degenerate H-He matter
- Interior – evolution – dynamo ?
- Fully convective layer ?

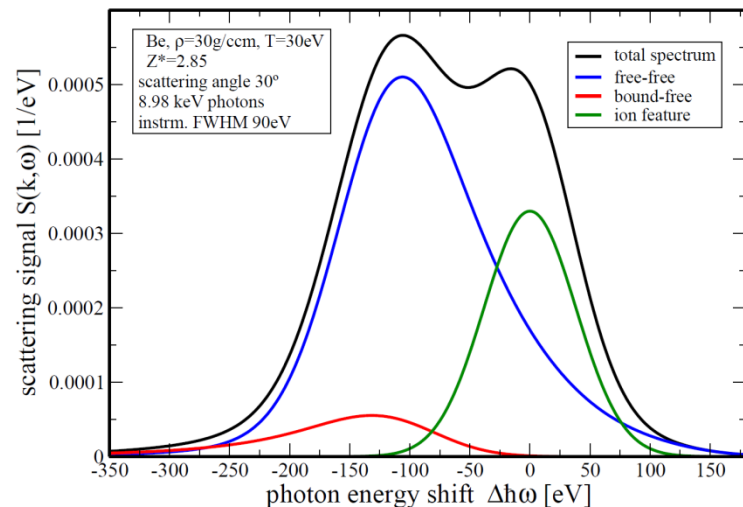
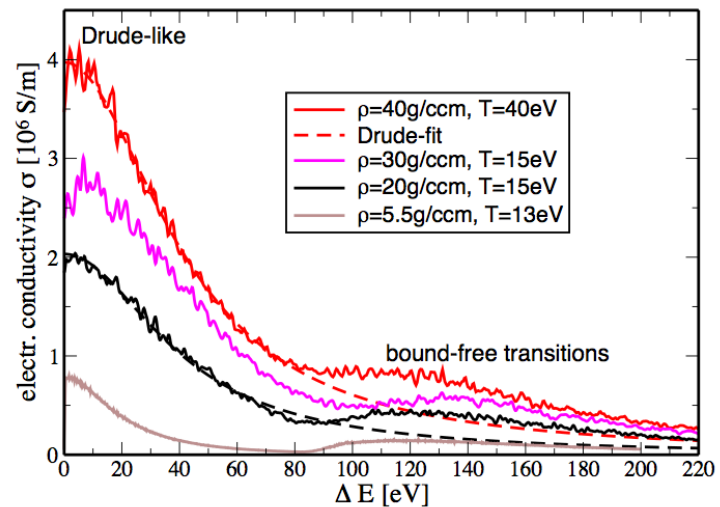


Gliese 229 B
1995, 18.8 Ly
M1 + T6 (50 AU)



A. Becker et al., ApJS 215, 21 (2014):
H-He EOS and one-layer interior models

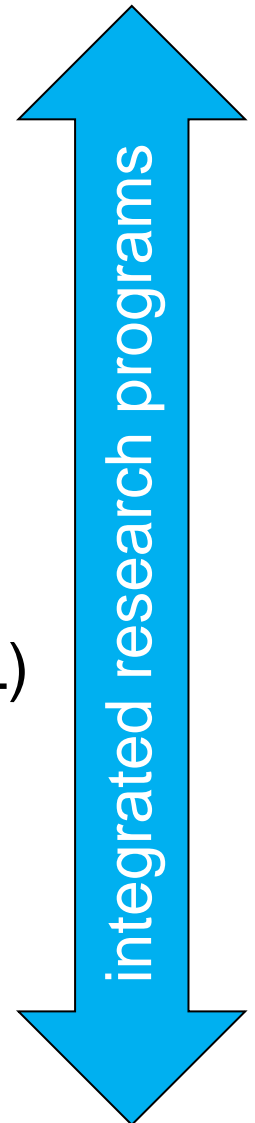
NIF shots will demonstrate collective XRTS in dense Be



DFT-MD: B. Witte

Summary & Outlook

- **Fundamental properties of WDM:**
 - ab initio simulations are an essential tool for
 - EOS data and high-pressure phase diagram
 - conductivities, viscosity
 - highly resolved XRTS spectra
- **Plasma diagnostics: infer plasma properties**
 - analyze DAC and shock wave experiments
 - analyze XRTS experiments (LCLS, European XFEL)
- **Application: planetary physics - understand**
 - diversity of solar/extrasolar planets
 - interior, evolution, magnetic field (dynamo)
 - **BDs: NIF shots D_WDM_XRTS_Be (17/11/07-08)**

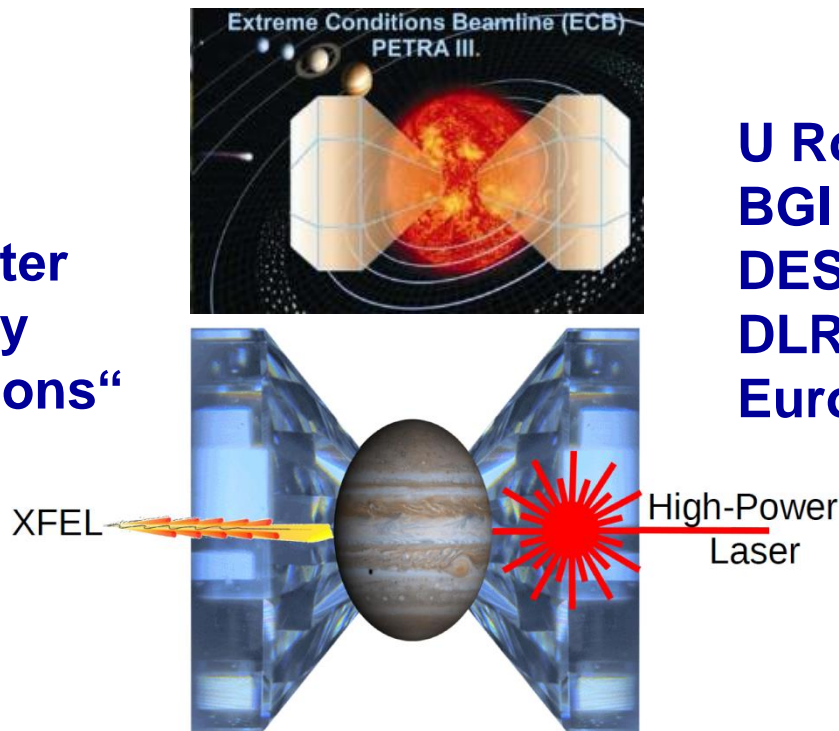


Upcoming Workshops & Conferences

16th International Conference on the Physics of Nonideal Plasmas (PNP-16)
September 24-28, 2018, Saint Malo

7th Joint Workshop on High Pressure, Planetary, and Plasma Physics (HP4)
October 10-12, 2018, DLR Berlin

**FOR 2440 „Matter
Under Planetary
Interior Conditions“**



**U Rostock
BGI Bayreuth
DESY
DLR Berlin
European XFEL**

Many thanks to

**Paul Grabowski
and HEDSC Team
for the invitation
and hospitality**

**Tilo Döppner and
the NIF Team for
the great shot day**

**All – for coming
and the interest**